A Study and Comparison of Various Nucleon-Nucleon (NN) Potential Models and Forms (Shapes)

1. Introduction

In 1953, Bethe [1] estimated that in the preceding quarter century more than hours of work had been devoted to the NN problem than to any other question in the history of humankind. NN interaction, since 1932 that Field was born, with neutron discovery by Chadwick, is in the heart of Nuclear Physics. In fact, during the first few decades of Nuclear Physics the term "Nuclear Force" was usually used as synonymous for nuclear force as a whole. They are good reason that why nuclear force play such an outstanding role. The interaction between two nucleons is basic for all of Nuclear Physics. The traditional goal of Nuclear Physics is to understand properties of atomic nuclei in terms of the "bare" interaction between pairs of nucleons. With starting of Quantum Chromo Dynamics (QCD), it became clear that the NN interaction is not fundamental. Nevertheless, even today, in any approach towards a nuclear structure problem, one assumes the nucleons to be elementary particles. The failure or success of this approach may then teach us something about the relevance of sub nuclear degrees of freedom. A large number of physicists, all over the world, have investigated the NN interaction for the past 70 years. This interaction is the empirically bestknown piece of strong interactions; in fact, for no other sample of strong force a comparable amount of experimental data has been accumulated. The oldest attempt to explain the nature of the nuclear force is due to Yukawa [2]. According to this theory massive bosons (mesons), mediate the interaction between two nucleons. Although, in the light of QCD, meson theory is not perceived as fundamental anymore, the meson exchange concept continues to represent the best working model for a quantitative Nucleon-Nucleon potential. Most basic questions were settled in the 1960's and 70's such that in recent years we could concentrate on the subtleties of this peculiar force [3].

2. A Concise Review of Nucleon-Nucleon Interaction

One can determine, with an introductory computation (e.g., by uncertainty principle), that two-nucleon force have the greatest contribution to the nuclear force and four- and further-body forces have not very great role in the nuclear calculations.

(2.1) Three Interaction Parts in Two-Nucleon System

(a) The long-range part ($r \geq 2\ fm$) : In the most of the potential models, it is considered as one-pion-exchange potential (OPEP) and is added to the other parts of potential as a tail for the long-range part. In the simplest state, it is as follows:

$$V_{OPEP}(r) = g^2 (\tau_1.\tau_2)\left[S_{12}\left(\frac{1}{(\mu r)^3}+\frac{1}{(\mu r)^2}+\frac{1}{\mu r}\right)e^{-\mu r}+(\sigma_1.\sigma_2)\frac{1}{3}\left(e^{-r\mu r}-\frac{4\pi}{\mu^3}\delta(r)\right)\right] \quad (1)$$

which $S_{12}=3(\vec{\sigma}_1.\hat{r})(\vec{\sigma}_2.\hat{r})-(\vec{\sigma}_1.\vec{\sigma}_2)$ is usual tensor operator and g is the value of coupling constant that obtains from experiments with mesons (meson-nucleon scattering). This potential has obtained some improvements (such as taking into account the difference between neutral and charged pions as well as that it is different for pp, nn, np interactions).

(b) The intermediate-range part $)21(fm \le r \le fm$: It comes mainly from the exchanges of scalar mesons (two pions and heavier mesons).

(c) The short-range part $)1(r \le fm$: It is given by the exchanges of vector bosons (heavier mesons-, and multi-pion-exchanges as well as QCD effects).

In some of the potential forms, various Feynman diagrams depend on the considered exchanges in each of the three mentioned parts are used.

(2.2) Deuteron, Only Bound State of Two-Body Systems

One way of the study of nuclear two-body interactions, is the using of a two-nucleon system such as deuteron (^2H nuclei). Of course, a comprehensive research requires that a general system of two-nucleon should build and this is constructed by scattering a nucleon from another one. Nevertheless, deuteron is necessary to understand some basic properties of nuclear force. Deuteron is only loosely bound state system of two-nucleon. From symmetry considerations, it is obvious that ^{3}S and$_1$ ^{3}D are its states. Non-zero Electric Quadruple $_1$ Moment for deuteron confirms the presence of D state in it, and leads to the introduction of tensor force. One can obtain [4]:

$$Q = \frac{\sqrt{2}}{10}\int_0^\infty uwr^2 dr - \frac{1}{20}\int_0^\infty w^2 r^2 dr \qquad (2)$$

As a way to measure a potential quality, one can insert the wave functions of S (u(r)) - and D (w(r)) – state, obtained from the special potentials, into above relation and then one may compared own results with experimental values.

(2.3) General Symmetry Properties of Two-Nucleon Hamiltonian

As a whole, the invariance of interaction under both the rotation of system (the isotropic property of space) and the translation of the origin of coordinate system (the homogeneous property of space) as well as time reversal, charge-independence, and chargesymmetry have been considered. In the above cases, the witnesses of violations (such as, the violation of the charge-independence and -symmetry) are exist [3] and therefore, almost all of the NN-potential forms consider these violations. From symmetry considerations, one can obtain tow-nucleon states as follows:

$$P_r P_\sigma P_\tau \psi(\vec{r},\sigma_1,\sigma_2,\tau_1,\tau_2) = -\psi(\vec{r},\sigma_1,\sigma_2,\tau_1,\tau_2) \qquad (3)$$

e.g., for np case, some states are as follows:

$$\begin{cases} S=0: {}_1P_1, {}_1F_3, {}_1H_5, {}_1K_7, {}_1M_9, \ldots \\ S=1: ({}_3S_1 - {}_3D_1), {}_3D_2, ({}_3D_3 - {}_3G_3), {}_3G_4, ({}_3G_5 - {}_3I_5), {}_3I_6 ({}_3I_7 - {}_3L_7), {}_3L_8, ({}_3L_9 - {}_3N_9), \ldots \end{cases} \qquad (4)$$

Refs. [4, 5, 6, 7, 8, 9, 10] are useful to give basic and general discussions on NN interaction.

(2.4) More about NN interaction

Generally, one can construct from two vectors the following combinations:

$$\begin{cases} \vec{A}.\vec{B} & (scalar) \\ \vec{A}\times\vec{B}, \vec{A} \pm \vec{B} & (vector) \end{cases} \qquad (5)$$

$$S_{ij} = \frac{1}{2}(A_i B_j + A_j B_i) - \frac{1}{3}\delta_{ij} \vec{A}.\vec{B} \quad (rank\ 2 spherical tensor)$$

For spin, isospin, space, momentum, and their combinations, one can also consider those cases that obey symmetry conditions. The general form of central potential is a linear combination from I, $\vec{\sigma}_1.\vec{\sigma}_2$, $\vec{\tau}_1.\vec{\tau}_2$, and $(\vec{\sigma}_1.\vec{\sigma}_2)(\vec{\tau}_1.\vec{\tau}_2)$ multiplying each operator in an appropriate radial function $V(r/a)$. The range parameter a, is in general different for various operators. Generally, these spin-isospin operators make a potential to be state dependent. The general forms of the central and non-central terms are as follows:

$$V_{central} = V_0(r) + V_\sigma(r)\vec{\sigma}_1.\vec{\sigma}_2 + V_\tau(r)\vec{\tau}_1.\vec{\tau}_2 + V_{\sigma\tau}(r)(\vec{\sigma}_1.\vec{\sigma}_2)(\vec{\tau}_1.\vec{\tau}_2)$$

$$\text{(6a)}\quad V_{nonncentral} = V_b(r)\vec{L}.\vec{S} + V_t(r)S_{12} + V_{\sigma\tau}(r)(\vec{L}.\vec{S})(\vec{\tau}_1.\vec{\tau}_2)$$

$$+ V_{b\sigma}(r)(\vec{L}.\vec{S})(\vec{\sigma}_1.\vec{\sigma}_2) + V_{b\sigma\tau}(r)(\vec{L}.\vec{S})(\vec{\sigma}_1.\vec{\sigma}_2)(\vec{\tau}_1.\vec{\tau}_2) + \ldots\ldots \quad \text{(6b)}$$

The matrix elements of the two-nucleon potential, for some operators, are:

$$\langle \vec{\sigma}_1.\vec{\sigma}_2 \rangle = \begin{cases} 1 & ;S=1 \quad (spin-triplet\ state) \\ -3 & ;S=0 \quad (spin-singlet\ state) \end{cases} \quad (7)$$

$$\begin{cases} I \\ \vec{\tau}_1.\vec{\tau}_2 \end{cases} \times V\left(\frac{r}{a}\right) \times \begin{cases} \sigma \\ \vec{r}^{1} \times \vec{\sigma} \cdot \vec{p}^{2} \\ \vec{\sigma}_1.\vec{\sigma}_2 \end{cases} \quad (spin-orbit)$$

(8)

$$S_{12} = 3(\vec{\sigma}_1.\hat{r})(\vec{\sigma}_2.\hat{r}) - \vec{\sigma}_1.\vec{\sigma}_2$$

$$\Rightarrow \langle \square' S j m, TM_T \left| \vec{L}.\vec{S} \right| \square S j m, TM_T \rangle = \frac{1}{2}\delta_{\square\square'} \left[j(j+1) - \square(\square+1) - S(S+1) \right] \quad (9)$$

$$\langle \square, S = 1, jm \left| S_{12} \right| \square', S = 1, jm \rangle = \quad (10)$$

$\square$ \ $\square'$	j	2
j		
2		

$\square$ \ $\square'$	$j-1$	$j+1$
$j-1$	$\frac{-2(j-1)}{2j+1}$	$\frac{6\sqrt{j(j+1)}}{2j+1}$
$j+1$	$\frac{6\sqrt{j(j+1)}}{2j+1}$	$\frac{-2(j+2)}{2j+1}$

The uncoupled radial Schrödinger equation (without the presence of Coulomb force) is: $\frac{d^2u}{dr^2} - \frac{j(j+1)}{r^2}u - \langle jSjm, TM_T \upsilon jSjm, TM_T \rangle u + k^2 u = 0$ (11)

The potential V is consist of a form function $V(r/a)$, a linear combination of various exchange operators, and the non-central operators $(L\square.S\square)$, $(L\square.S\square)^2$, S_{12}. Asymptotic solutions are as follows: $r \to 0 \Rightarrow u(r) = \begin{cases} r^{\square+1} \\ r^{-\square} \end{cases}$; $r \to \infty \Rightarrow u = -\frac{1}{k} A_\square \sin\left(kr - \frac{1}{2}\square\pi - \frac{1}{2} + \delta_\square\right)$ (12) r

As soon as one finds an asymptotic solution, the solution for all r will be obtained by a numerical integration, and by having phase shifts, one can obtain a potential from above Schrödinger equation. For couple-states (without the presence of the Coulomb force), we have as well:

$$\begin{cases} \frac{d^2u}{dr^2} - \frac{j(j+1)}{r^2}u + F_2(wr) + uG + (Hr)(wr) + wH = 0 \\ \frac{d^2w}{dr^2} - \frac{j(j+1)}{r^2}w + F_2(wr) + uG + (Hr)(wr) + wH = 0 \end{cases} \quad (13a)(13b)$$

The ground state of the deuteron is a special case of above equation with $k^2 = -\gamma^2$ (bound state) and j=1. u and w are now the radial functions for ^3S - and ^3D - states, respectively. Because two partial-wave channels are coupled, thus an incoming wave in the either $\square = j-1$ or $\square = j+1$channel is scattered into either $\square = j-1$ or $\square = j+1$ channel. Therefore, we have two phase shifts (proper phases) δ^{α}_{j}, δ^{β}_{j} and a mixing parameter (ε). In the presence of the Coulomb potential, a Coulomb phase shift adds as well, and therefore the problem becomes a little complicated [5].

On the other hand, if the kinetic energy of the center of mass of two-nucleon system is larger than the necessary amount to produce a meson, inelastic reactions become possible (see, Fig.1).

Because the mass of lightest meson ($\pi_{\pm}$) is about $140 MeV/c^2$, therefore we expect, when the bombarding energy is upper than threshold, some of the kinetic energy in the system be transmitted to pion. Along with the increase of energy, the excitement of the internal degrees of freedom of nucleon and the production of the other particles become more and more probable. Inelastic scattering shows the wastage of flow from incident channel and probability amplitude is no longer conserved. Such a condition is described by complex scattering potential and other relativistic effects become important. Therefore, two-nucleon Schrödinger equation is no longer sufficient. At the time of the discussion of different potential forms, we will speak further about this subject.

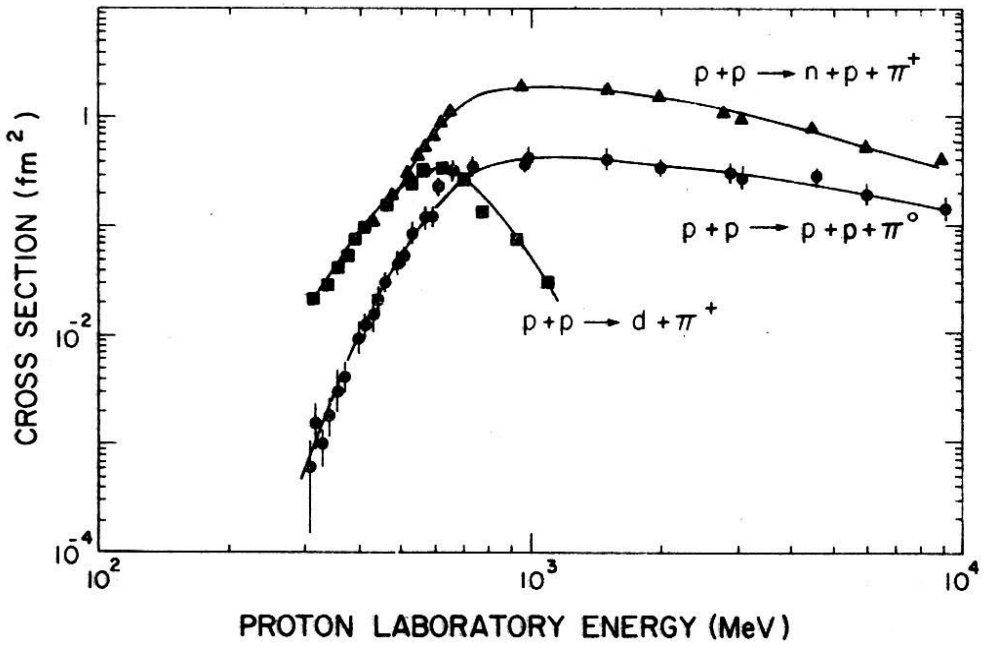

***Fig. 1**. Charge-dependent cross section for pion production in the np scattering through the reactions: $p+p \rightarrow d+\pi^+$, $p+p \rightarrow p+p+\pi^+$, and $p+p \rightarrow p+p+\pi^0$ (quoted from Ref. [11]).*

(2.4.1) Effective range formalism for low-energy scattering: Semi-classic arguments may be used to show that at very low energy, the S state alone contributes to scattering and then, as energy increases, even higher angular momentum states start participating in the process. This is a consequence of the short range of the NN force. If this range is denoted by a and the momentum by p, then the maximum angular momentum state that can be affected by the scattering potential is obviously given by pa. Equating the square of this quantity with $\ell(\ell+1)$, we can very easily evaluate the energy at which a given ℓ begins to acquire importance. Very simple computation places this energy for the $\ell=1$ state at approximately 10 MeV. For np scattering below this energy, we have the following expressions (e.g., see, Sec. II.C in Ref. [4], or Sec. 9.a in Ref. [5]):

$$k \cot\delta = -\frac{1}{a} + \frac{1}{2} r_0 k^2 - P k^4 r_0^3 \qquad (14)$$

By the time that the term in k^4 becomes important $(E \geq 10 MeV)$, P- and D-waves begin to come into the scattering so that it is not easy to unravel the k^4 dependence of $k\cot\delta$ for the S-wave phase shift. Consequently, the really useful region of energy for the above relation is that in which the first two terms suffice. In the case where the Coulomb potential is present (pp scattering), an approximate effective range expansion is as follows (for instance, see, Sec. IV.C, or Sec. 9.b in Ref. [5], or see, Ref. [12]):

$$C^2 k \cot\delta + 2k\eta\, h(\eta) = -\frac{1}{a} + \frac{1}{2} r_e k^2 - \mathrm{Pr}_{e3} k^4 \qquad (15)$$

$$^2(\overline{e^{2\pi\eta}\pi\eta}\,;\ \eta = \overline{Me_2{}^2 k}) \qquad (15a)$$

where $C = {}_2 1)\ (2\square$

and $$h(\eta) = -\gamma - \log\eta + \eta^2 \sum_{M=1}^{\infty} \left[M\left(M^2+\eta^2\right)\right]^{-1}, \quad r = 0.577 \qquad (15b)$$

Using above relations and three low-energy ^{1}S phase shifts, one can obtain the parameters a_0, r_e, P (e.g., for a special potential).

(2.4.2) A brief on scattering in momentum-space: For many calculations associated with NN interaction, it is appropriate to express the Schrödinger equation as an integral equation in the momentum-space. The extracting of Lippmann-Schwinger and Low equations and also several properties of T-matrix are useful. Separable potentials, separable expansions from arbitrary potentials, inverse scattering problem, N/D equations, and other related topics are discussed in this formulation.

(2.4.3) A brief on relativistic scattering: We can consider the modification of the LippmannSchwinger equation necessitated by the kinematics of relativity. At first glance, such modifications might seen to be of little relevance to the problem of NN scattering below the first inelastic threshold since the energy in the center of mass system is always a modest fraction of the nucleon rest mass. This is not the case, however, due to the ubiquitous shortrange repulsion familiar from phenomenological descriptions of the NN interaction using local potentials. In field theoretical discussions of the NN interaction, this repulsion is associated with the exchange of ρ, ω, and φ mesons (observed VNN coupling constants suggest that the isoscalar ω meson provides the most a significant vector meson exchange contribution to the force at short distances that this exchange yield repulsion is reasonable by analogy with exchange of a more familiar neutral vector particle, the photon, between particles of like charge. in the case of ω meson exchange, the baryon number assumes the role of the "strong charge"). This strong repulsion forces the two-nucleon wave function in S states to decrease rapidly at distances less than almost 0.5 Fermi and thus build high momentum components into the wave function at all scattering energies. There is no reason to believe that these high momentum components can be described adequately by the nonrelativistic scattering equations. Within the context of phenomenological descriptions of the NN interaction, the inadequacies of the non-relativistic approach are of little importance since the parameterizations of the interaction currently employed do have sufficient flexibility to provide a quantitative fit to experimental data. To the extent that our goal is to provide a quantitative description of NN scattering in

terms of the exchange of bosons with coupling constants and masses determined from other experiments, using non-relativistic scattering equations are justified only so long as they represent a numerically reliable alternative to a fully relativistic description of the scattering process.

In the absence of a complete theory of strong interactions, the investigation of suitable approximate relativistic equations is to some extent speculative. Thus, one may be begin by modifying the Lippmann-Schowinger equation slightly in order to satisfy an unambiguous requirement of each relativistic theory that the scattering amplitude should incorporate relativistic unitary along the elastic cut. While the resulting equation is a familiar relativistic extension of the L-S equation discovered independently by many investigations, it emphasizes that it is not in no sense unique (e.g., see, Sec. VI.A in Ref. [4], pages 64 on).

3. Nucleon-Nucleon Interaction Models

(3.1) The Models Based on QCD

The aim of such models is to connect hadronic interactions with the fundamental underlying theory of nuclear strong interaction (QCD). The objective is to interpret the hadron-hadron processes in terms of quark and gluon degrees of freedom.

Due to its nonperturbative character in the low-energy regime, QCD cannot be solved exactly for the problem under consideration. Chiral Perturbation Theory (CHPT), the skyrme model, and Nambu-Jona-Lasinio (NJL) type are examples of this type of approach. These models describe characteristic phenomena that are observed in Nucleon-Nucleon, Pion-Nucleon, and Pion-Pion scattering quite well but quantitatively they fail. Common features of "QCDinspired" models that detract from their appeal are cumbersome mathematics, large numbers of parameters, and a limitation in applications essentially to very low energies (the references about NN interaction in QCD framework are given in the last Refs. of Sec. 6). Therefore, if a quantitative and sensible description of data is sought, preference is often given to date to phenomenological approaches such as with the boson exchange models and inverse scattering theory. We have two subsets of this model along with main characteristic features in the following lines:

1) Gluon and quark exchange plus pauli-repulsion between like quarks in overlapping nucleons: (a) Gluon exchange based on constituent quark model plus one gluon exchange potential- this has not a good description for reasonable distances (because of the confinement of non-color singlet). (b) Pauli repulsion related to minimum energy to excite a nucleon (i.e., to move a quark into a different state) of 300 MeV. (c) Quark exchange between nucleons can exchange their charge (n→pand at same time p→n). (d) It gives a reasonable (semiquantitative) description of short-range repulsive part of the NN potential (and may be intermediate-range).

2) Chiral symmetry and chiral Perturbation theory: (a) It is based on chiral symmetry of QCD lagrangian (quarks of opposite helicity are indistinguishable and do not couple to each other except for their masses). (b) Chiral symmetry is spontaneously broken (because QCD prefers quark-quark pairs with positive ones) and in consequence, low mass modes (theoretically, zero) of the "quark condensate" are called "Goldeston bosons" (pions, kaons, etc.). This constrains the lagrangian for processes involving nucleons and pseudoscalar mesons. In other words, in strong interactions, the transition from the "fundamental" to "effective" level happens through a phase transition that takes place around $\Lambda_{QCD} \approx 1 GeV$ via the spontaneous breaking of chiral symmetry, which generates pseudoscalar Goldston bosons. Therefore, at low energies ($E < \Lambda_{QCD}$), the relevant degrees of freedom are not quarks and gluons, but pseudoscalar mesons and other hadrons. Approximate chiral symmetry is reflected in the

smallness of the masses of the pseudoscalar mesons. The effective theory that describes this scenario is known as CHPT. (c) Chiral symmetry is also violated by the (small) quark masses, so Goldston bosons are not massless totally. Nevertheless, one can extend the interaction in small parameters like to make definite predictions (CHPT in above).

(3.2) Effective Field Theory (EFT) Approach

It is wholly like all of the effective field theories, in the sense that they are low energy approximations to some "high" theories. generally: (a) It describes nature on different, separate length and mass scales without using underlying theory expect for its symmetries; in other words, the basis of the EFT concept is the recognition of different energy scales in nature, each energy level has its characteristic degrees of freedom. As the energy increases and smaller distances are probed, new degrees of freedom become relevant and must be included. Conversely, when the energy drops, some degrees of freedom become irrelevant and they are frozen out. (b) Example: chiral symmetry. (c) In the context of NN interaction, EFT means applying all symmetries (including chiral symmetry) of QCD lagrangian but not explicitly taking into account underlying degrees of freedom like pions or guarks. This gives a most general lagrangian, which contains many parameters one can constrain with data, here, to make any assumption of simplicity about the lagrangian and consequently to assume renormalizability are not allowed. The lagrangian must include all possible terms, because this completeness guarantees that the effective theory is indeed the low energy limit of the underlying theory. Now, this implies that we faced with an infinite set of interactions. To make the theory manageable, one needs to organize a perturbation expansion. Then, up to a certain order in this expansion, the number of terms that contribute is finite and the theory will yield a well-defined result.

More about CHPT and EFT: A systematic improvement in the ability of the model to reproduce the NN data is observed when stepping up the orders of the chiral expansion. One of the extended models (NNLO) of CHPT describes the np phase shifts well up to about 100 MeV; over this energy, the discrepancies are present in the some partial waves. In spite of the fact that this case (NNLO) and the most recent chiral NN potential represent great progress as compared with earlier ones, however, for meaningful applications in microscopic nuclear structure, further quantitative improvements are necessary. If one believes to the basic ideas of EFT, then at low energies, CHPT is as fundamental as QCD at high energies. Moreover, due to its perturbative arrangement, CHPT can be calculated order by order. Therefore, here, one may have what one is asking for: a basic theory that is amenable to calculation. Therefore, CHPT has probably the potential to overcome the discrepancy between theory and practice that has beset the theoretical research on the nuclear force for so many years.

(3.3) Almost full phenomenological models

General form of potential allowed by symmetries like rotation, translation, isospin, and… that generally, has the following features: (a) somewhat in the same spirit as EFT, but much older and restricted to space-time and isospin symmetries. (b) Four important terms are central potential V(r), spin-spin (SS) interaction, spin-orbit (LS) interaction , and tensor (S_{12}) interaction. (c) Each term occurs twice, once without isospin dependence, and once with $\tau_1 . \tau_2$ (which measures total isospin of NN combination). The latter terms are responsible for charge-changing pion exchange etc. (d) The tensor term is important for long-range part of potential and arises "naturally" from pion exchange (QED analogy: magnetic dipole-dipole). In these potential models, intermediate- and short-range parts are determined wholly in a phenomenological way and for long-range part, one pion exchange potential is often used. The examples of these potentials are Hamada-Johnston potential, Yale group potential, Reid

potentials (Reid68, Reid68-Day, Reid93), Urbana potentials (e.g.,$Urbana V_{14}$), Argonne potentials (e.g., $Argonne V_{14}$, $Argonne V_{18}$), etc.

(3.4) Boson Exchange Models

The potential acting between a pair of particles due to the exchange of a meson has a range of the order of the meson Compton wavelength that is inversely proportional to the meson mass. Since the π meson is the lightest boson that can be exchanged between a pair of nucleons, the OPEP determines the long-range part (beyond the pion Compton wavelength) of the two-nucleon potential. If one wants information on the two-nucleon potential at intermediate- and short-ranges, one is then faced with the computation of the potential arising from the exchange of the heavier bosons and two, three,… pions. Since this computation is comparatively more difficult, thus at the potentials constructed based on symmetries (e.g., Breit and coworkers potential), it is determined phenomenologically; while at the meson theory of the two-nucleon potential, these exchanges are considered explicitly. It is understood that multi-meson systems most often have strongly correlated resonance states behaving as a single boson. It is therefore speculated that some of these multi-meson resonances, when exchanged between two nucleons may dominate the intermediate- and short-range behavior of the two-nucleon potential. The potential computed in this way is called the one-boson-exchange potential (OBEP). Besides the exchange of one π meson, also other exchanges have been explicitly considered in the OBEP. A main difference amongst workers on the meson theoretic two-nucleon potential lies in their manner of treatment of the two-pion system. An approach in which the effect of the two-pion system is parameterized through one or two isoscalar (T=0), scalar (J=0) mesons is one such treatment. In another development of the theory, the effect of the S-state of the two-pion system is parameterized through the scattering length and effective range (for instance, see, chapter VIII in Ref. [4]). In yet another attempt the effect of two-pion continuum is considered in more detail and the resultant potential taken into account explicitly. Various authors also differ in the details of their method of computing the potential. Broadly speaking, conventional field-theoretical techniques and the dispersion theoretic method are the two principal methods of solving the problem that we do not express these methods in details here. A review article about OBEP is advised to the reader in Ref. [13].

Therefore, in other words, the boson exchange potentials are based on effective field theory and are expanded to nucleon-nucleon, pion-nucleon, and pion-pion interactions. These models do not any reference to QCD, but the baryon and meson fields have been considered as the asymptotic states that absorb all effects from quark-gluon dynamics. The discovery of the spin-one or vector mesons ρ and ω with the masses around 770-780 MeV was provided a progress and led to the expansion of the OBE potentials. In these models, the unrelated single exchange contributions of the pseudoscalar mesons π)138(, η(549) and the vector mesons ρ(769), ω(783) as well as the scalar meson δ)983(have been considered and iterated into the scattering equation. In addition, the two-pion exchange associated with the fictional scalar sigma meson with the masses around 400-800 MeV was demonstrated. The core region was finally parameterized by the phenomenological form factors related to the meson-nucleon vertices. Finally, those form factors formed the substructure of QCD. Such OBE potentials provided the first quantitative approximation of data. Many models of these potentials exist that each have owns definite and separable features. It is now known that these are the standard NN potentials, of course. A few examples are Nijmegen, Paris, and Bonn potentials. Broadly speaking, in this quark-antiquark pair (=meson) exchange model, we have the following features: (a) It is similar to quark exchange (just reverse direction of one quark). (b) It gives a very good description of many aspects of NN potential. (c) It is preferred because meson states

are color-neutral and have relatively low mass (larger range). (d) It studies OPEP and generalizes to other mesons- so far only model that gives perfect agreement with data, especially for long-range part.

4. Various Forms (Shapes) of Two-Nucleon Potential

(4.1) Basic Potentials

As already mentioned, the range of the nucleon-nucleon interaction is divided to the three parts: the short-range $(r \leq 1fm)$, the intermediate-range $(1fm \leq r \leq 2fm)$, and the longrange $(r \geq 2fm)$. For the long-range part, one-pion exchange (OPE) has usually been considered. The short-range part has often been discussed phenomenologically; in some models, form factors are introduced to regularize the potential at the origin whereas in other models a hard core is used. The first logical approach to describe the intermediate-range region was to include the two-pion exchange contributions (the examples of the two-pionexchange (TPE) potentials are given in Refs. [14, 15]). However, these TPE models, did not give a satisfactory description of the NN scattering data, mainly due to a lack of a sufficient spin-orbit force. Gammel, Christian, and Thaler [16] hinted the necessity of a spin-orbit force, when they tried to fit all of the data available at that time with a phenomenological velocitydependent (local) potential as:

$$V = V_C(r) + V_T(r) S_{12} \quad (16)$$

for each of four spin and isospin combinations and they failed.

In 1975, the simultaneous construction of the purely phenomenological potentials by Gammel-Thaler [17] and the semi-phenomenological Singell-Marshak potential [18], where both models introduced phenomenological spin-orbit potentials, began. The Gammel-Thaler model gave a good fit to scattering data up to 310 MeV. The Singell-Marshak model, consisting of the TPE Gartenhaus potential [19] together with a phenomenological spin-orbit force, was successful up to 150 MeV. Okubo-Marshak showed that the most general twonucleon potential, considering symmetry conditions, is as follows:

$$V(r\vec{}, \sigma\vec{}_1, \sigma\vec{}_2, \tau\vec{}_1, \tau\vec{}_2) = V_0(r) + V_\sigma(r)(\sigma\vec{}_1 . \sigma\vec{}_2) + V_\tau(r)(\tau\vec{}_1 . \tau\vec{}_2) + V_{\sigma\tau}(r)(\sigma\vec{}_1 . \sigma\vec{}_2)(\tau\vec{}_1 . \tau\vec{}_2)$$

$$+ V_{LS}(r)(\tau\vec{}_1 . \tau\vec{}_2) + V_{LS\tau}(r)(L\vec{} . S\vec{})(\tau\vec{}_1 . \tau\vec{}_2)$$

$$+V_T(r)S_{12}+V_{T\tau}(r)S_{12}(\tau_1.\tau_2) \quad (17)$$
$$+V_Q(r)Q_{12}+V_{Q\tau}(r)Q_{12}(\tau_1.\tau_2)$$
$$+V_{pp}(\sigma_1.p)(\sigma_2.p)+V_{pp\tau}(r)(\sigma_1.p)(\sigma_2.p)(\tau_1.\tau_2)$$

where $L.S$ and Q_{12} are spin-orbit- and quadratic spin-orbit- operators, respectively.

which $Q_{12} = \frac{1}{2}\{(\sigma_1.)(\sigma_2.)+(\sigma_2.)(\sigma_1.)\}$ (18)

Twelve terms are given by twelve radial functions $V_0(r)$, ... We can obtain the V(r) 's from our knowledge from the basic nature of the nuclear force such as the meson exchange and or from the semi-empirical procedure by fitting some assumed forms of the radial dependence to experimental data. When our understanding of QCD is fully developed in the future, it will be possible to determine these functions from first principles. The first four terms of the Eq. (17) are the central force terms and in this case, L and S are the good quantum numbers. In the presence of the other terms, two-nucleon system is invariant only in the combined space of L and S labeled by J;

$$V_{Spin-Orbit}(r)=V_{LS}(r)\,L.S+V_{LS\tau}(r)(L.S)(\tau_1.\tau_2) \quad (19)$$

The reason for these two terms comes from the possibility that the radial dependence of the isospin-dependent and of the isospin-independent parts may be different from each other, for example as the result of different mesons being exchanged. The six and the seven terms are the tensor force. The ninth and the tenth quadratic spin-orbit terms enter only when there is momentum dependence in the potential. The last two terms are often dropped since for elastic scattering, they can be expressed as a linear combination of other terms. Their contributions therefore cannot be determined using elastic scattering, for which most of our information on NN interaction is derived.

Then, soon after, better potential forms were constructed. Some examples are Hamada-Johnston [21], Yale [22], and the various hard- and soft-core models constructed by Reid [23]. Before going into the treatment of other potentials, it is useful to mention that most of the experimental elastic phase shifts are extracted from the pp and np differential cross sections. In these models, the data are fitted up to the energy range 0-350 MeV, because, as already mentioned, in higher energies (with the threshold 270 MeV) the pion production and other relativistic effects become important and the Schrödinger two-nucleon equation is therefore no longer sufficient. Hamada-Johnston and Yale group (Breit & et. al.) potentials reproduce all the two-body scattering data (including the polarization parameters) as a function of energy over the energy range of several hundred MeV. The Yale potential was especially designed to reproduce the phase shifts in various two-nucleon states as smooth functions of energy. As a first step, the phase parameters (phase shifts, and the mixing parameter in the case of coupled states) were determined as a function of energy by direct fit to all the scattering and polarization data. The setting up of the potential with its parameters adjusted to reproduce the phase parameters may be regarded as the second step in this type of work. The first step, namely the determination of the phase parameters as a function of energy has been practiced very efficiently by several groups of workers including the Yale- [24], Livermore- [25], and other- teams. The

actual procedure, now almost standardized, entails expressing the scattering amplitude as the sum over partial waves up to a certain maximum orbital angular momentum $\square_{max}$ (the usual value chosen for $\square_{max}$ is more or less 5). The contribution of all higher partial waves is then taken to be represented by the one-pionexchange contribution (OPEC) to the scattering amplitude. The Yale group took the OPEP as a given component of the potential and then determined the rest of the potential by fitting the energy-dependence phase parameters up to $\square_{max}$.

(4.2) Hamada-Johnston (HJ) potential

The general form of HJ potential, for short- and long-range parts, is as follows:

$$V = V_C + V_T S_{12} + V_{LS} L\square.S\square + V_{LL} L_{12} \qquad (20a)$$

where $S_{12} = 3(\sigma\square_1 .r\hat{}\,)(\sigma\square_2 .r\hat{}\,) - (\sigma\square_1 .\sigma\square_2)$ and $L_{12} = \left(\delta_{\square j} + \sigma\square_1 .\sigma\square_2\right)\square^2 - (\square\square.S\square)^2$, respectively; also:

$$V_C = 0.08(13\mu)(\tau\square_1 .\tau\square_2)(\sigma\square_1 .\sigma\square_2)Y(x)\left[1 + a_c Y(x) + b_c Y_2(x)\right]$$

$$V_T = 0.08(13\mu)(\tau\square_1 .\tau\square_2)Z(x)\left[1 + a_t Y(x) + b_t Y^2(x)\right]$$

(20b)

$$V_{LS} = \mu G_{\square S} Y^2(x)\left[1 + b_{\square S} Y(x)\right]$$

$$V_{LL} = \mu G_{x-2} Z(x)\left[1 + a_{\square\square} Y(x) + b_{\square\square} Y_2(x)\right]$$

which μ, x, and M are the pion mass in MeV, the internucleon distance measured in units of the pion Compton wavelength (1.415 fm), and the nucleon mass (is taken to be 6.73μ) respectively; and also:

$$Y(x) = \frac{e^{-x}}{x}; \quad Z(x) = \left(1 + \frac{3}{x} + \frac{3}{x^2}\right)Y(x) \qquad (20c)$$

The values of the parameters a_c, b_c, a_t, b_t, … as determined from the detailed fit to the scattering data are given in the original Ref. [21]. These radial shapes of the potential are used outside the hard core of the radius $x_c = 342.0$. The HJ potential as originally proposed would lead to bound triplet ($\square = j$)-odd states which are known to be non-existent. There the triplet ($\square = j$)- odd state potential has subsequently been modified as follows: It has been defined as -0.26744μ in the region $x \le x_c = 487.0$ and by above relations for $x > 0.487$. The values of the binding energy, electric quadratic moment, and D state probability of deuteron, have been determined by this potential with the values $2.226 MeV$, $0.285 fm^2$, and 6.97% respectively [21].

(4.3) Yale group (Breit and his collaborations) potential

This potential is very similar to the HJ potential. The OPEP is explicitly used and the quadratic spin-orbit coupling is written in a somewhat different form. The entire two-nucleon potential is expressed as:

$$V = V_{OPEP} + V_C + V_T S_{12} + V_{LS} L\square.S\square + V_L \left[Q_{12} + (L\square.S\square)^2 \right] \quad (21a)$$

$$\left[Q_{12} + (L\square.S\square)^2 \right] = -(L\square.S\square)^2 - L\square.S\square + L\square^2 \quad (21b)$$

$$V_{OPEP} = \left(\frac{12g^2}{M\mu} \right) \frac{\mu}{12} \tau\square.\tau\square_2 \left[\sigma\square_1.\sigma\square_2 + S_{12} \left(1 + \frac{3}{x} + \frac{3}{x^2} \right) \right] \frac{e^{-x}}{x} \quad (21c)$$

which V_{OPEP} forms the NN interaction in the distances larger than almost 3 fm, and x, μ, and M are the quantities defined in the context of the HJ potentials, and the coupling constant g is given by setting $g^2/94.014 =$ in the singlet-even states and unity elsewhere. The neutralpion mass is used for singlet-even and triplet-odd states (i.e., T=1 states), whereas for singletodd and triplet-even states (i.e., T=0 states), a weighted mean of charged- and neutral- pion masses is used in proportion 2-to-1. The hard-core radius is taken to be $x_c = 0.35$. All depths V_C, V_T,… are in the following form:

$$V = \sum_{n=1}^{7} a_n \frac{e^{-2x}}{x^n} \quad (21d)$$

The values of the parameters in the various spin-parity states and for the different types of V (i.e., V_C, V_T,…) are given in the original Ref. [22]. Also, it is useful to mention that HJ and Yale potentials are OPEP for $L > 5$, and Yale potential sets $V_{LS} = 0$ for $J > 2$.

(4.4) Reid68 and Reid-Day Potentials

Both HJ and Yale hard-core potentials have some failures in the many-body calculations. A two-nucleon potential with a softer repulsive core would be more efficient. The most important different feature of the Reid potential from the HJ and the Yale potential is that Reid determined the potential, in each two-nucleon state, independent of the other states. It may appear that this approach would produce one potential for each of the infinite number of two-nucleon states and hence the data fitting in this way would become patently meaningless. In practice, however, this is not so. Since the highest energy (almost 350 MeV) considered in the analysis is rather low, Reid confined himself to a few two-nucleon states, namely, those with $J \leq 2$. In the singlet- and uncoupled-triplet-states (which $L = J$), Reid used a central potential, and for the coupled triplet states, he used a potential having central, tensor, and spin-orbit ($L\square.S\square$ and not quadratic components); i.e.:

$$V = V_C(r) + V_T(r) S_{12} + V_{LS}(r) L\square.S\square \quad (22)$$

In the OPEP g^2 was taken to be 14 and a short-range interaction was subtracted from its tensor-part to remove the x^{-2}, x^{-3}, behavior at small x. The lack of the soft-core versions is that the potentials are not regular at origin and have r^{-1} singularity yet. At intermediate distances the potential was represented by sums of convenient Yukawas of the form e^{-nx}/x where n is an integer. The short-range repulsion was expressed by means of hard (infinitely hard) and soft

(Yukawa) cores [23]. In 1981, B. D. Day [26] expanded the Reid68 soft-core potential up to $J = 5$ which this expansion was of course not based on fundamental underlying discussions about NN interaction.

(4.5) Super-Soft-Core Potential

This pp plus np potential contains the π-, ρ-, and ω-exchange contributions where the coupling constants are taken from other sources. The other important intermediate-range contributions to the NN force are parameterized phenomenologically through OBE potential functions with 32 free ranges and amplitudes. The potential contributions are regularized at the origin by step-like functions which also serve to construct the short-range phenomenological cores, whence the name super-soft-core potential [27]; this model is an improved version of an earlier super-soft-core model by the same group [28]. **(4.6) Funabashi Potentials**

These potentials are constructed from the π, η, ρ, and ω OBE potentials. Also, included are the contributions of two-scalar mesons and δ , σ, the masses of which were fitted to the scattering data. The potential contains the standard OBE part and a retardation part. The off-energy-shell effects coming from the retardation albeit of little importance to the twonucleon system are expected to play an important role in many-nucleon systems. The potentials were evaluated in coordinate space for the sake of feature investigations regarding the influence of off-energy-shell effects in finite nuclei. The various treatments of the inner region in these potentials are a hard core, a Gaussian soft core, and a velocity-dependent core. In each case, an attractive spin-orbit core is included to improve the triplet P phase shifts. Furthermore, all potentials are regularized by means of a step-like cut-off function [29]. (**4.7) Nijmegen Group Potentials**

The Nijmegen group considered baryon-baryon and baryon-antibaryon interactions. In first instance, few potentials were constructed by this group and then partial-wave-analysis (PWA) [30, 31], of the experimental scattering data were performed. The knowledge obtained of the PWA was then applied to construct the new and improved potentials. In the NN (pp or np) potentials, for the nuclear part of the potential, charge-dependence is adopted. For exchanged mesons and for the nucleons, averaged isomultiplet masses are used such as the average pion mass $m = (2m_+ + m_0)/3 = 138.4 MeV$, the nucleon mass

$M = (M_p + M_n)/2 = 938.93 MeV$, etc. In other words, in these potentials, the mass discrepancies are taken into account. Because of the short-range parameterization, the Nijmegen potentials remain in contact with QCD. Generally, these potentials can be grouped into the following several classes [32].

(4.7.1) Hard-core (HC) potentials: This class was given from 1975 to 1979, and almost gives a good description of data. The examples of these potentials are NijmD [33, 34] and NijmF[35].

(4.7.2) Soft-core (SC) potentials: Nijm78 potential [36] was published in 1987 and afterward(s) the update Nijm93 potential [37] was constructed from it. The Nijm78 potential is a nonrelativistic OBE in the configuration space and besides the six mentioned meson before, (i.e., π, η, ρ, ω, δ, σ), the η)958(, φ(1020), and S(993), are also included. The dominant J=0 parts of the pomeron (or many-gluon exchanges) and the tensor Regge Trajectories (f, f', A_2) are taken into account as well. The internal region regularizes by means of an exponential form factor. The 13 model parameters were fitted to the phase-shift-error-matrices of the 1969 Livermore [38] analyses. These model parameters can be checked by meson-nucleon coupling constants and cutoffs obtained from other sources. The hyperon-nucleon version of this Nijm78 potential was published in 1989 and used to baryon-antibaryon as well, which gave a good

description of different reactions. One of the attractive features of this potential is that the configuration-space version and the momentum-space version are exactly equivalent, that is at the cost of having a minimal form of non-locality.

(4.7.3) Extended-soft-core (ESC) model: Here an important improvement is performed on the soft-core OBE model inspired by besides soft OBE potentials, also the contributions from two-meson exchanges diagrams ,...),,(ππππρπε and from one-pair and two-pair diagrams (ππ,πρ,πε,...) . The latter are generated through pair-vertices (ππ,πρ,πε,...) . The meson-pair vertices are except for a few, all fixed by heavy saturation.

(4.7.4) Nijmegen partial-wave-analysis (PWA): About two decades ago, the Nijmegen group embarked on a program to improve NN phase shift analysis [30] substantially. To achieve to this goal, they first constructed the database, i.e. they scanned the world NN database (all data in the energy range 0-350 MeV laboratory energy published in regular physics journals between 1955 to 1992) and eliminated all data that had either a very high or a very low χ^2. Of the 2078 word pp data below 350 MeV, 1787 survived the scan, and of the 3446 np data 2514 survived. Then (second), they introduced sophisticated semi-phenomenological model assumptions into the analysis. Namely, for each of the lower partial waves (J≤)4a different energy-dependence potential was adjusted to constrain the energy-dependent analysis. The phase shifts were obtained using these potentials in a Schrödinger equation. From these phase shifts, the predictions for the observables were calculated including the χ^2 for the fit of experimental data. Thus, strictly speaking, the Nijmegen analysis is a potential analysis; the final phase shifts are the one predicted by the "optimized" partial-wave potentials. In the Nijmegen analysis, each partial wave potential includes the short-range part and long-range part with the separation line at r=1.4fm . The long-range potential V_L $(r>1.4\ fm)$is constructed from an electromagnetic part V_{EM} a nuclear part V : $_N$

$$V_L = V_{EM} + V_N \qquad (23)$$

The electromagnetic interaction can be written as follows:

$$V_{EM}(pp) = V_C + V_{VP} + V_{MM}(pp) \qquad (23a)$$ for proton-proton scattering and as:

$$V_{EM}(np) = V_{MM}(np) \qquad (23b)$$

For neutron-proton scattering, where V denotes a Coulomb potential (which takes into $_C$ account the lowest order relativistic corrections to the static coulomb potential and includes contributions of all two-photon exchange diagrams); V_{VP} is the vacuum polarization potential, and V_{MM} the magnetic moment interaction. The long-range nuclear potential V , includes the $_N$ contributions of the one-pion-exchange (OPE) tail (the coupling constant f , being one of the $_\pi$ used parameter to minimize the) multiplied by a factor M / E (M is the nucleon mass and E is the center of mass energy) and the tail of the heavy-boson-exchange (HBE) contribution of the Nijmegen potential [36], (V_{HBE}), enhanced by a factor of 1.8 in singlet states; i.e., :

$$V_N = \frac{M}{E} \times V_{OPE}(f_\pi, m_\pi) + f_{med}(S) \times V_{HBE} \qquad (23c)$$

with $f_{med}(S=0)=1.8$ and f_{med} 0.1)1($S=$ = where S denotes the total spin of the two-nucleon system. The energy-dependent factor M / E (with $E = M\sqrt{^2 + q^2}$ and $q^2 = MT_{lab} / 2$) takes into account in a "minimal" way, damping the non-relativistic OPE at higher energies. One of the

fact in the NN scattering is that we encounter with four different pseudovector coupling constants at the pion-nucleon-nucleon vertices, i.e.: $f_{pp\pi^0}$, $f_{nn\pi^0}$, $f_{np\pi^-}$, $f_{pn\pi^+}$. For the combinations that really occur in the OPE potential, they used the following definitions:

for $pp \to pp$: $f_p^2 \equiv f_{pp\pi^0} f_{pp\pi^0}$

for $np \to np$: $f_0^2 \equiv - f_{nn\pi^0} f_{pp\pi^0}$ (23d)

for $np \to pn$: $2 f_c^2 \equiv f_{np\pi^-} f_{pn\pi^+}$

Considering charge symmetry, $f_p^2 = f_0^2$, whereas in the charge-independence case, $f_p^2 = f_0^2 = f_c^2$.

For pp scattering, OPE potential can be written as follows:

$$V_{OPE}(pp) = f_p^2 V(m_{\pi^0}) \quad (23e)$$

and for np scattering is:

$$V_{OPE}(np) = -f_0^2 V(m_{\pi^0}) + (-1)^{I+1} 2 f_c^2 V(m_{\pi^+}) \quad (23f)$$

where I denotes total isospin and V (m) for a large amount of r is given as follows:

$$V(m) = \frac{1}{3}\left(\frac{m}{m_s}\right)^2 \frac{e^{-mr}}{r}\left[(\sigma_1 \cdot \sigma_2) + S_{12}\left(1 + \frac{3}{mr} + \frac{3}{(mr)^2}\right)\right] \quad (23g)$$

where scale mass m introduces to make the pseudovector coupling constant f, dimensionless $_s$ and is usually considered as charged-pion mass. The short-range potentials)4.1($r \leq fm$ are energy-dependent square-wells (see, Fig. 2 and 3 in Ref. [30]). The energy dependence of the depth of the square well is parameterized in terms of three parameters per partial wave. For the states with J≤4 , there are a total 39 such parameters (21 for pp and 18 for np) plus the pion-nucleon coupling constants ($f_{\pi^\pm}$, f). In the Nijmegen np analysis, the I=1 np phase $_0$ shifts are calculated from the corresponding pp phase shifts (except in ^1S where an $_0$ independent analysis is conducted) by applying corrections due to electromagnetic effects and charge dependence of OPE. Thus, the np analysis determines ^{1}np(S_0) and the I=0 states, only. In the combined Nijmegen pp and np analysis [30], the fit for 1787 pp data, and 2514 np data below 360 MeV, available in 1993, results in the "perfect" $\chi^2 / datum$ =99.0.

(4.7.5) High-quality (HQ) potentials: As already mentioned, in the Nijmegen partial-waveanalysis of the NN scattering data, these data are described with$\chi^2 / N_{data} \approx 1$. In this manner, the quality of a potential can be described via the difference from this value. The high quality (HQ) potential is defined for giving $\chi^2 / N_d < 1.051$. These HQ potentials are NijmI, NijmII, and Reid93, that all of those have the best valueχ^2 / N_d =03.1.

The soft-core potential Nijm78 [36], was a starting point in the construction of the high quality NN potentials. The NijmI potential contains the momentum-dependence terms, which in configuration space give rise to a non-local structure ($\Delta\phi(r) + \phi(r)\Delta$) to the potential (where Δ is Laplacian). In totally local potential NijmII, momentum-dependent terms are eliminated (in

other words, all non-locality in each partial wave removed, i.e., $\phi(r) = 0$) and the Reid93 potential is an update of the old Reid (Reid68) potential. These three potentials have the same number of the fit parameters as PWA [30] and give a χ^2_{min} nearly similar to PWA93 (i.e., close to the expectation value); hence, the differences among e.g., the phase parameters of these models, provide an indication for the systematic error in the Nijmegen partial-wave analysis. The NN potentials can be written in either the configuration space or the momentum space:

$$(\Delta + k^2)\psi = 2M_r V\psi \qquad (24)$$

(where (non)relativistic refers to the kinematics. For relativistic kinematics the relation between the center-of-mass energy E and center of mass momentum squared k^2 reads $E = \frac{k^2}{2M_r}$ whereas for relativistic kinematics it reads $E = \sqrt{k^2 + M_1^2} + \sqrt{k^2 + M_2^2} - M_1 - M_2$).

Writing the potentials as $V = \sum_{i=1}^{6} V_i P_i$, the six operators in configuration space are as follows:

$$P_1 = 1, \quad P_2 = \vec{\sigma}_1.\vec{\sigma}_2, \quad P_3 = S_{12} = 3(\vec{\sigma}_1.\vec{r})(\vec{\sigma}_2.\vec{r}) - (\vec{\sigma}_1.\vec{\sigma}_2), \quad P_4 = \vec{L}.\vec{S}$$

$$P_6 = \tfrac{1}{2}(\vec{\sigma}_1 - \vec{\sigma}_2).\vec{L} \quad P_5 = Q_{12} = \tfrac{1}{2}\left[(\vec{\sigma}_1.\vec{L})(\vec{\sigma}_2.\vec{L}) + (\vec{\sigma}_3.\vec{L})(\vec{\sigma}_1.\vec{L})\right], \qquad (25)$$

where these operators are also frequently referred to as the central, tensor, spin-spin, spinorbit, quadratic spin-orbit, and anti-symmetric spin-orbit operators, respectively. For identical-particle scattering, the P_6 can not contribute, whereas V_6 vanishes when charge dependence is assumed (which is usually the case for NN potential models). In general, each potential form V_i in configuration space is a function of r^2, and of the operators p^2 and L^2. In most approaches, one only keeps the dependence on r^2, while the p^2 dependence (when included) is often present in a linear way in the central potential V_1. The inclusion of the Q_{12} operator was found to be necessary, because otherwise it was impossible to describe simultaneously the $^1S_0$ and $^1D_2$ phase shifts using the same static potential. The presence of the Q_{12} in the potential can to a certain extent be simulated by introducing non-local $\sum_{i=1}^{6} V_i P_i$ potentials. In the expansion $\sum V_i P_i$, the potential forms V_i are generally assumed to be the same in all partial waves. The potential differences between the partial waves are dictated by the differences in the expectation values of data, the Reid68 potential, however, is based on a quite different approach. Rather than having six potential forms V_i which are the same for all partial waves, now each partial wave is parameterized separately. The potentials forms V_i, therefore, not only depend on r^2 and L^2, but also on S^2 and J^2. The potential models in which each partial wave is parameterized separately, is known as Reid-Like.

In the momentum space, introducing $\vec{k} = \vec{p}_f - \vec{p}_i$, $\vec{q} = \frac{1}{2}(\vec{p}_f + \vec{p}_i)$, $\vec{n} = \vec{q} \times \vec{k}$ where $\vec{p}_i$ and $\vec{p}_f$ are the initial and final momentum, respectively, the operators, equivalent to (25) are as follows:

$$\begin{cases} P_1 = 1, P_2 = \sigma_1 . \sigma_2, P_3 = (\sigma_1 . k)(\sigma_2 . k) - \frac{1}{3} k^2 (\sigma_1 . \sigma_2) \\ P_4 = -2i (\sigma_1 + \sigma_2) . n, P_5 = (\sigma_1 . n)(\sigma_2 . n), P_6 = -2i (\sigma_1 + \sigma_2) . n \end{cases} \quad (26)$$

The potential forms V_i in the momentum space are functions of k, q, n, and energy. Although above operators are an adequate set of six linearly independent operators, the Q_{12} operator, in configuration space, is not the exact Fourier transformation of the $(\sigma_1 . n)(\sigma_2 . n)$ operator, in momentum space. On the other hand, if one wants both the momentum space and the configuration space versions produce exactly the same phase shifts and bound states, the configuration space version should be an exact Fourier transform of the momentum-space version, and vice versa. This implies that one should use the inverse Fourier transformation of the Q_{12} operator; i.e., the potential contribution $(\sigma_1 . n)(\sigma_2 . n) V_5(k^2)$ is to be replaced by:

$$P_5' = [(\sigma_1 . q)(\sigma_2 . q) - \frac{1}{3} q^2 (\sigma_1 . \sigma_2)] - \frac{1}{4} [(\sigma_1 . k)(\sigma_2 . k) - \frac{1}{3} k^2 (\sigma_1 . \sigma_2)] \quad (27)$$

where $P_5 V_5(k^2) - P_5' \int_{\infty}^{k} dk'^2 V_5(k^2)$. Other restrictions imposed on the momentum-space potential forms V_i in that case are that they should not depend on the energy, while the q dependence should be of second order at most. When the potentials are evaluated in the momentum space and then Fourier transformed to configuration space, they are usually first regularized to move the singularities at the origin. This can be achieved by introducing a form factor $F(k^2)$. A typical Fourier transform, encountered in transforming the momentum-space potentials to the configuration space, then reads:

$$\int \frac{d^3k}{(2\pi)^3} \frac{e^{ik \cdot r}}{\vec{k}^2 + m^2} (\vec{k}^2)^n F(\vec{k}^2) \equiv \frac{m}{4\pi} (-m^2)^n \phi^n(r) + \frac{m}{4\pi} (-\nabla^2)^n \phi_C^0(r) \quad (28)$$

The results for various frequently used choices are the following: (i) No form factor, $F(k^2) = 1$. This yields the familiar Yukawa potential:

$$\varphi_C^0(r) = \frac{e^{-mr}}{mr} \qquad (29)$$

and the singularities at the origin are still present. (ii) Monopole form factor, $F(k^2) = (\Lambda^2 - m^2)/(\Lambda^2 + k^2)$, normalized such that at the pole $m(F - 1) = 0$. This yield:

$$\varphi_C^0(r) = \left[e^{-mr} - e^{-\Lambda r}\right]/mr \qquad (30)$$

(iii) Dipole form factor, $F(k^2) = (\Lambda^2 - m^2)^2/(\Lambda^2 + k^2)^2$, yielding:

$$\varphi_C^0(r) = \left[e^{-mr} - e^{-\Lambda r}\left(1 + \frac{\Lambda^2 - m^2}{2\Lambda^2}\Lambda r\right)\right]/mr \qquad (31)$$

(iv) Exponential form factor, $F(k^2) = e^{-k^2/\Lambda^2}$, yielding: $\varphi_C^0(r) = e^{\frac{m^2}{2\Lambda^2}}\left[e^{-mr}\,\mathrm{erfc}\left(\frac{m}{\sqrt{2}\Lambda} - \frac{\Lambda r}{\sqrt{2}}\right) - e^{mr}\,\mathrm{erfc}\left(\frac{m}{\sqrt{2}\Lambda} + \frac{\Lambda r}{\sqrt{2}}\right)\right]/2mr$ (32a)

where erfc(x) is the complementary error function:

$$\mathrm{erfc}(x) = \frac{2}{\sqrt{\pi}}\int_x^\infty dt e^{-t^2} \qquad (32b)$$

using explicitly the definition (28), the Fourier transforms for the tensor and spin-orbit potentials can be simply expressed in terms of derivatives of the central function, i.e.,

$$\varphi_{T_0}(r) = 3\left(\frac{1}{mr}\right)^2 \frac{dr}{d}\left(\frac{1}{mr}\frac{dr}{d}\right)\varphi_{C_0}(r) \qquad (33a)$$

$$\varphi_{SO0}(r) = -\frac{m}{2}\frac{1}{r}\frac{dr}{d}\varphi_{C0}(r) \qquad (33b)$$

In order to ensure regularity at the origin for the tensor and spin-orbit functions, one must choose at least the dipole or exponential form factor. In that case, the tensor function also vanishes at the origin, as it should.

The presence of explicit momentum-dependent terms in the potential in configuration space potential give rise to non-local structure in the potential in configuration space. The q^2 terms pose on difficulties for the configuration-space potential as long as they are linear in q^2. The typical Fourier transform of such a term is given by:

$$\int \overline{(2d\pi_3 k)}\,\overline{k\square\, e^{+ik.r\square}} \qquad \left(q\square_2 + \_1\,\overline{k\square_2}\right)\overline{F(k\square_2)} = -\,m\,\left|\left[\Delta\phi 2M(r_r) + \phi 2M(r_r)\,\Delta_.\right]\right| \tag{34}$$

$$_3\ _2\quad m_2\left|\left(\qquad 4\quad \right)\right.\qquad\qquad 4\pi\lfloor$$

where $\varphi(r) = M_r\,\phi_C^0(r)$. It is known how to handle such a $(\Delta\phi + \phi\Delta)$ term [41]. The absence of $q\square^2$ terms in the momentum-space potential will result in a radial local configuration-space potential.

The NijmI, NijmII, and Nijm93 potentials [37], which are based the original Nijm78 potential [36], are regularized with the exponential form factor, whereas the update Reid68 potential (Reid93) is regularized using a dipole form factor.

The structure of the high quality (HQ) potentials

(a) one-pion-exchange potential (OPEP): In these models, in the OPE part, the mass differences between neutral-pion and charged-pion exchange are explicitly considered (the mass distinction between the neutral- and charged-pion indicate that the isovector np and pp potentials are different, and also charge-independence breaks; it is however assumed that the pion-nucleon coupling constants obey charge-independence here). Almost, all other potentials appeared in the literatures have used a mean pion mass. In these models, the isovector np phase parameters are larger in magnitude than the corresponding pp phase parameters. By explicitly including the pion-mass difference, this exactly becomes inverse that is a feature of the present potentials here. Defining:

$$V(m) = \qquad\qquad _{2}$$

$$\left(\left|\left\backslash\right.\right.\qquad \overline{\qquad\qquad} \qquad mm_{\pi_\pm}\left\backslash\right|\right|\qquad\qquad \_ \qquad\qquad m\left|\left\lceil\left\lfloor\varphi_T^0(m)S_{12} + {}^{1}3\varphi_C^1(m,r)\left(\sigma\cdots_1.\sigma\cdots_2\right)\right|\right|\right\rceil \tag{35a}$$

$$\text{where}\quad \varphi_C^1)(4)()(r = \varphi_C^0 r - \pi\delta^3 m^{r\square} \tag{35b}$$

The Eq. (35b), is in the absence of a form factor; in this case, Eq. (35b) is still holds, but the δ-function contribution is smeared out. The OPE potential for pp scattering is given by:

$$V_{OPE}(pp) = f_\pi^2\,V(m_{\pi^0}) \tag{36a}$$

whereas for np scattering, it becomes:

$$V_{OPE}(np) = -\,f_\pi^2\,V(m_{\pi^0}) \pm 2\,f_\pi^2\,V(m_{\pi^\pm}) \tag{36b}$$

where plus (minus) sign corresponds to total isospin I=1(0).

(b) Nijm93, NijmI, and NijmII potentials: The basic functions are the one-boson-exchange (OBE) potential functions with momentum-dependent central terms and exponential form functions. The meson exchanges that included are those due to pseudoscalar mesons (π,η,η'), vector mesons (ρ,ω,φ), and scalar mesons $(a_0\,,,f_0\,\varepsilon)$. a , corresponds to the $_0\delta$, and f_0 to the S^*. Furthermore, the dominant J=0 parts of pomeron, and of the f_2 , f_2', and a_2 tensor-meson trajectories, are also included where they give rise to Gaussian potentials. The meson

propagators, including the exponential form factor, and for the pomeron-type exchanges are respectively given by:

$$\Delta\left(k^2,m^2,\Lambda^2\right)=\frac{1}{k^2+m^2}e^{-k^2/\Lambda^2} \qquad (37a)$$

$$\left(k^2,m^2_p\right)=M^1_{p2}e^{-k^2/4m_{2p}} \qquad (37b)$$

where m_p and M_p are the pomeron and proton masses, respectively. The different potential forms are evaluated in the momentum space and the resulting expressions are essentially those of Ref. [36], with the following differences: (i) taken explicitly into account the proton and neutron mass difference, (ii) the differences between the neutral- and charged- pion, and between the neutral- and charged- ρmeson are explicitly included, (iii) the quadratic spinorbit operator of the potential in momentum space is adjusted to include the P_5' contribution as in Eq. (37a). The effect of the first modification is rather small. The second modification (as well as the first) implies that charge independence is broken in the non-OBE part of the potential as well. For pp scattering the potential includes only neutral-meson exchange, [$V_{pp}=V(neutral)$], whereas for np scattering it includes neutral-meson exchange, depending on the total isospin as in Eq. (36b), (2)([$V_{np}=-V\ neutral\ \pm\ V\ charged$)]. This distinction replaces the factor $(\tau_1.\tau_2)$ in the old Nijm78 [29] potential. Finally, the third modification, as mentioned before, demonstrates the equivalence of a potential in both momentum space and configuration space that is a unique feature of these Nijmegen potentials. Comprehensive discussion about these potential forms is found in Refs. [36, 37].

(c) Regularized Reid potential: A disadvantage of the original Reid68 potential is that at the time of construction of it, the quality of the np data was very poor. Another disadvantage is that the Reid68 potential has 1/ *r* singularity in all partial waves (i.e., when the potential is evaluated in the momentum space and then Fourier transformed into configuration space, first of all, the singularities at the origin must be regularized) and this can be achieved by introducing a form factor $F(k^2)$ (here, a dipole form factor).

As in the case for the original Reid68 potential, the OPE potential is explicitly included, while the mass difference between the neutral-pion and charged-pion, as in Eq. (36b), is furthermore included now. For the pion-nucleon coupling constant at the pion pole, $f_\pi^2=075.0$, and for the dipole cutoff parameter, $\Lambda=8m_\pi$, are chosen. In the OPE potential (Eq. 35a), φ_C^1 is used only for the S waves; for all other waves, it was found that using φ_C^0 instead of φ_C^1 is convenient (we note that φ_C^1 up to a modified δ function, and that this modified δ function is screened by the centrifugal barrier for all these other partial waves, except the S waves). Starting with this OPE potential, the potential in each partial wave can now be extended by choosing a convenient contribution of central, tensor, and spin-orbit functions with arbitrary masses and cutoff

parameters, here $\overline{m}=(m_{\pi^0}+2m_{\pi^+})/3$, $\Lambda=8\overline{m}$. For simplicity, the following notations were defined:

$$Y(p)=p\overline{m}\varphi_c^0(p\overline{m},r)$$

$$Z(p)=p\overline{m}\varphi_T^0(p\overline{m},r) \qquad (38)$$

$$W(p)=p\overline{m}\varphi_{SO}^0(p\overline{m},r)$$

where p is an integer and φ_{SO}^0 and φ_T^0 are given by Eq. (33). For coefficients multiplying these functions, A_{ip} and B_{ip} are used for the isovector potentials and for the isoscalar np $^1S_0$ potentials, respectively. The index i, subsequently labels the different partial waves. For the total potential in a particular partial-wave, one should of course add the appropriate OBE potential as given by Eq. (35) and (36). For instance, for the non-OPE parts in the isovector singlet partial waves $(I=1,S=0,L=J)$, the potentials are:

$$V_{pp}(^1S_0)=A_{12}Y(2)+A_{13}Y(3)+A_{14}Y(4)+A_{15}Y(5)+A_{16}Y(6) \qquad (39a)$$

$$V_{np}(^1S_0)=B_{13}Y(3)+B_{14}Y(4)+B_{15}Y(5)+B_{16}Y(6) \qquad (39b)$$

$$V(^1D_2)=A_{24}Y(4)+A_{25}Y(5)+A_{26}Y(6) \qquad (39c)$$

$$V(^1G_4)=A_{33}Y(3) \qquad (39d)$$

$$V(^1J_1)=V_{pp}(^1S_0) \quad for\ J\geq 6 \qquad (39e)$$

where the distinction between the pp and np $^1S_0$ potentials is necessary because of the wellknown breaking of charge independence in the pp and np $^1S_0$ partial waves. The coefficients A_{ip} and B_{ip} are to be fitted. The presence of the two-pion range piece $A_{12}Y(2)$ in the pp $^1S_0$ potential is purely coincidental, and is only included to improve the quality of the fit. A similar term in the np $^1S_0$ is much less effective, and so is leaving out [37].

The predicated values of the quantities by these potentials Nijm93, NijmI, NijmII have a good agreement with experimental ones.

(4.7.6) Optical potentials: Below the threshold for pion-production, the NN-potentials are real. When one wants to describe the inelasticities in the scattering above these thresholds, then either one has to go to a complicated coupled channel description or one has to introduce an optical NN potential:

$$V=V_R-iV_I \qquad (40)$$

From the Nijmegen partial-wave-analysis (PWA), it determines that the purely real potentials work at most up to $T_{lab}=500MeV$ reasonably. The optical potentials of this group were constructed by adding, to real HQ-potentials, the same imaginary part as was used in their PWA of the np data below $T_{lab}=500MeV$. These optical potentials have not good results for all partial waves. In Fig. 2, the phase shifts as determined in a preliminary PWA of all np data below 1GeV, are given. For the $^1S_0$-phase the description is good up to 1 GeV; for the $^1D_2$ wave, one notices quite large differences. However, after refitting, the modified NijmI optical potential (NijmI (mod)) is got, which give a very good fit to the $^1D_2$-phase shift up to 1 GeV.

$^1S_0$ $^1D_2$

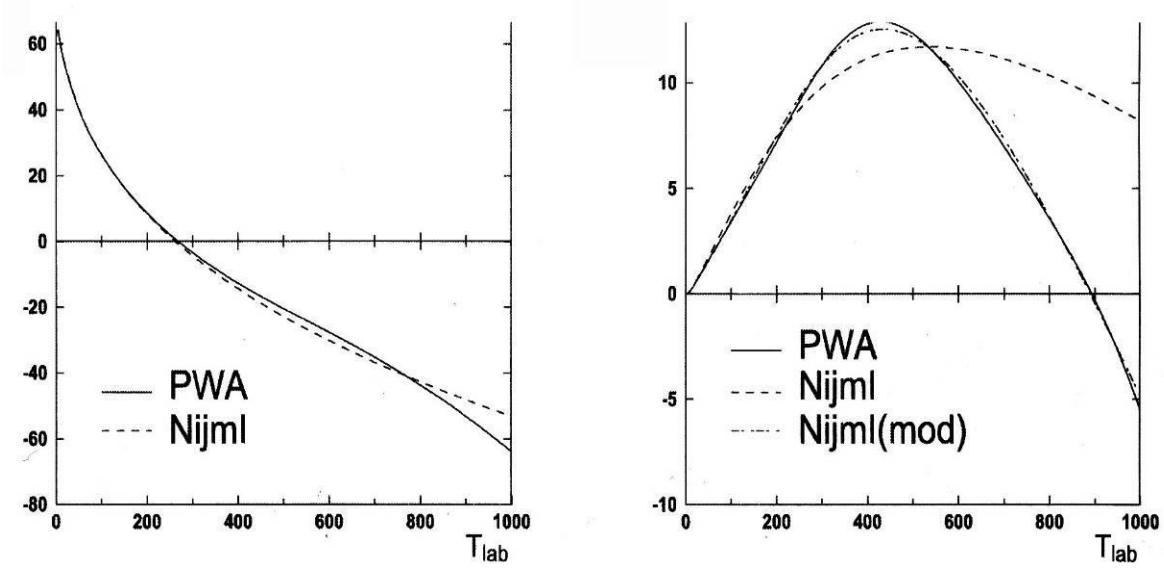

Fig. 2. *The phase shifts* $^1S_0$ *(left), and* $^1D_2$ *(right) for optical NijmI potential and a modified version of it (quoted from page 8 of Ref. [32]).*

(4.8) Paris Group Potential

The original Paris potential [42] was obtained from pion-pion phase shifts and pionpion interaction using scattering relations, with taking into account two-pion-exchange (TPE) contribution for nuclear force. The π exchange and ω exchange were also included. Fitting to the phase-shift-error-matrices of the 1969 Livermore [38] and pp, np scattering data, required all 12 parameters. In 1980, the parameterized version of it [43], including a set of the Yukawa functions (12 local functions), provided a phenomenological representation of the Paris potential. Expect for very low region, this model gives a good description of the pp scattering data. In 1985, a modified separable representation of the Paris NN potential in the $^1S_0$ and $^3P_0$ states was performed [44], which was to remedy shortcomings of an earlier parameterization in the $^1S_0$ and $^3P_0$ partial waves. In particular, this latter parameterization does not lead to the unphysical bound states at very large negative energies as encountered previously. Still, it provides a good approximation of the on-shell as well as off-shell properties of the Paris potential.

(4.9) Urbana Potential

The UrbanaV_{14} potential is a fully phenomenological potential where 14 is the number of the different potential types (central, spin-spin, tensor, spin-orbit, centrifugal, centrifugal spin-spin, and general dependence on isospin). In other words, NN scattering data indicate the occurrence of terms belonging to the following eight operators:

$$O_{ijp=1,18} = 1, \vec{\sigma}_i.\vec{\sigma}_j, \vec{\tau}_i.\vec{\tau}_j, (\vec{\sigma}_i.\vec{\sigma}_j)(\vec{\tau}_i.\vec{\tau}_j), S_{ij}, S_{ij}(\vec{\tau}_i.\vec{\tau}_j), (\vec{L}.\vec{S})_{ij}, (\vec{L}.\vec{S})_{ij}(\vec{\tau}_i.\vec{\tau}_j) \quad (41a)$$

The above operators are obtained by fitting the NN phase shifts up to 425 MeV in S, P, D, F waves, and deuteron properties. The following six phenomenological potentials:

$$O_{ijp=9,14} = L^2, L^2(\vec{\sigma}_i.\vec{\sigma}_j), L^2(\vec{\tau}_i.\vec{\tau}_j), L^2(\vec{\sigma}_i.\vec{\sigma}_j)(\vec{\tau}_i.\vec{\tau}_j), (\vec{L}.\vec{S})^2, (\vec{L}.\vec{S})^2(\vec{\tau}_i.\vec{\tau}_j) \quad (41b)$$

(six "quadratic L" terms) are relatively weak, and chosen in order to make many-body calculations with this operator simpler. In general,

$$\upsilon_{ij} = \sum_p \upsilon^p(r_{ij}) O_{ij}^p \tag{42}$$

where $\upsilon^p(r_{ij})$ are functions of the interparticle distance r , and $_{ij}O_{ij}^p$ are conveniently chosen operators. In this model, NN interaction has been written as follows:

$$V_{ij} = \sum_{p=1,14} \left(\upsilon_\pi^R(r_{ij}) + \upsilon_I^p(r_{ij}) + \upsilon_S^p(r_{ij})\right) O_{ij}^p \tag{43}$$

(from now on, instead of the functions associated with above 14 operators, we use c, σ, τ, στ, t, tτ, b, bτ, q, qσ , qτ, qστ, bb, bbτ respectively).

The one-pion-exchange $\upsilon_\pi^p(r_{ij})$ is non-zero only for $p=\sigma\tau, t\tau$:

$$\upsilon_\pi^{\sigma\tau}(r) = 3.488 \frac{e^{-0.7r}}{0.7r}\left(1 - e^{-cr_2}\right) \tag{44a}$$

$$\upsilon_\pi^{t\tau}(r) = 3.488 \left(1 + \frac{3}{0.7r} + \frac{3}{(0.7r)^2}\right) e^{-0.7r} \left(1 - e^{-cr_2}\right)^2 = 3.488 T_\pi(r) \tag{44b}$$

The $1/r$ and $1/r^3$ singularities of OPE potential are removed, and the cutoff parameter c is determined by fitting the phase shifts. Green and Haapakoski [46] have recommended the $(1 - e^{-cr_2})^2$ cutoff arguing that it simulates the effect of ρ-exchange interaction. Here, the $\upsilon_\pi^{\sigma\tau}(r)$cutoff is purely Yukawa shaped, because the quark models suggest that nucleon is not a point source, and so the two-nucleon interaction should not have a $1/r$ behavior at small r. The $\upsilon_I^p(r_{ij})$is attributed to second-order OPE transition potentials. So its radial dependence should approximately be given by $T_\pi^2(r)$. Thus, in this model, $\upsilon_I^p(r_{ij})$is used as:

$$\upsilon_I^p(r_{ij}) = I^p I_\pi^2(r) \tag{45}$$

This choice of υ_P also makes it simpler to introduce effects of three-nucleon interactions [41]. The strengths I are determined by fitting the phase shifts. ^{p}

Traditionally the short-range interaction $\upsilon_S^p(r_{ij})$ is attributed to ω-and ρ- exchange, and taken to have a Yukawa shape. However, since the believed size of nucleon is at least of the order of the Compton wavelength of ω- and ρ-mesons, the Yukawa shape will be very much modified. Hence, in the UV_{14} interaction model, $\upsilon_S^p(r_{ij})$ is taken to be a sum of two Woods-Saxon potentials:

$$\upsilon_S^p(r) = S^p W(r) + S'^p W'(r) \tag{46}$$

$$W(r)=\left[\left(1+\exp\left(\frac{r-a^{R}}{}\right)\right)\right]^{-1} \quad (46a)$$

$$W'(r)=\left[\left(1+\exp\left(\frac{r-a'R'}{}\right)\right)\right] \quad (46b)$$

It is possible to obtain reasonable fits to the scattering data with $S'^{p}=0$ for all p expect b and bτ. The spin-orbit potential in I=1 states has to have a smaller range than that of the central core to fit the scattering data. Hence, the $W'(r)$ terms are needed for p=b and bτ. The parameterization of UV_{14} potential has similarities with that used by Hamada and Johnston [21], and by Brussel et al. [47]. The values of the parameters are determined by fitting the neutron-proton phase shifts obtained by Arndt et al. [48], by energy-dependent analysis, taking into account: (i) the obtained phases by energy-independent analysis, (ii) a more recent analysis by Arndt [49] of the mixing ε_1 in the $^3S_1 - {}^3D_1$ channel, and (iii) the recent analyses of Bugg et al. [50], particularly in regions where energy-dependent and independent analysis give different phases. These phase shifts up to 425 lab energy are fitted. In the opinion of this group, not because if one wants to correct for effects of relativistic kinematics it may be useful to start from a non-relativistic potential that indeed fits the scattering data. The model parameters and comprehensive description for this model are given in Ref. [45].

(4.10) Argonne Group Potentials

(4.10.1) Argonne V_{14} potential: The basic potential of Argonne group [51] is similar to the *Urbana*V_{14} potential. It was fitted to the 1981 phase shifts analysis of Arndt and Roper (an update of the analysis of Ref. [48]) for the np scattering data in the 25-40 MeV energy range. Next to OPE and a 14-parameter representation of TPE, the short-range part of the *Argonne*V_{14} potential is represented by a Woods-Saxon potential using 16 parameters. A main reason to construct this new V_{14} model was to have a phase-equivalent standard of comparison for V model. This includes operators that represent all possible processes with $_{28}$ $N\Delta\pi$ or $\Delta\Delta\pi$ vertices. The description of the Nijmegen PWA at very low energy region is bad, this is not surprising in view of which the model was fitted to the np data with $T_{lab} > 25MeV$. Also, the 50 MeV bin are not described too well. Still, in the 25-350 MeV region the *Argonne*V_{14} model provides an important over the *Urbana*V_{14} model.

(4.10.2) Argonne V_{18} potential: The *Argonne*V_{18} potential [52] is a high quality NN potential, with explicit charge dependence and charge asymmetry. This model has a chargedependent part with fourteen operators that is an updated version of the *Argonne*V_{14} potential (these 14 operators are just those in the *Urbana*V_{14} potential, see, Eq. (41a)). Three additional charge-dependent and one charge-asymmetry operators are added along with a complete electromagnetic interaction. The potential is fitted directly to the Nijmegen pp and np scattering database, low-energy nn scattering parameters, and deuteron binding energy. With 40 adjustable parameters, it gives a χ^2 per datum of 1.09 for 4301 pp and np data in the range 0-350 MeV.

The *Argonne*V_{18} potential is written as a sum of an electromagnetic (EM) part, a one-pionexchange (OPE) part, and intermediate- and short-range phenomenological part:

$$\upsilon(NN)=\upsilon^{EM}(NN)+\upsilon^{\pi}(r_{ij})+\upsilon^{R}(r_{ij}) \quad (47)$$

The EM interaction is the same as that used in the Nijmegen partial-wave-analysis [30], with the

addition of short-range terms and finite-size effects. For pp scattering, one- and two-photon Coulomb terms, the Darwin-Foldy term, vacuum polarization, and the magnetic moment interaction, each with an appropriate form factor, are included: $\upsilon^{EM}(pp) = V_{C1}(pp) + V_{C2} + V_{DF} + V_{MM}(pp)$ (48)

$$V_{C1}(pp) = \alpha' \frac{F^c(r)}{r} \qquad (48a)$$

$$V_{C2} = -\frac{4M\alpha}{} \left[\left(\nabla^2 + k^2\right) F_c r(r) + F_c r(r) \left(\nabla^2 + k^2\right)\right] \approx -\alpha M \alpha_p' \left[F_c r(r)\right] \qquad (48b)$$

$$V_{DF} = -\frac{\alpha}{4M_p^2} F_c(r) \qquad (48c)$$

$$V_{DP} = \frac{2\alpha}{3\pi} \alpha' F_c r(r) \int_1^\infty dx \; e^{-2m_e rx} \left[1 + \frac{1}{2x^2}\right] \frac{\sqrt{x^2 - 1}}{x^2} \qquad (48d)$$

$$V_{MM}(pp) = -\frac{4M\alpha}{} \mu_p^2 \left[\frac{2}{3} F_\delta(r) \sigma_i \cdot \sigma_j + \frac{}{} F r_t(3r) S_{ij}\right] - \frac{2\alpha M}{} \mu_p^2 (4\mu_p - 1) F_{ls} r(r) L \cdot S \qquad (48e)$$

The Coulomb interaction includes an energy dependence through the $\alpha' \equiv (2k\alpha / M_p \upsilon_{lab})$ [53], which is significantly different form α at even moderate energies ($\approx$ 20% difference at $T_{lab} = 250\text{MeV}$). The vacuum polarization and two-photon Coulomb interaction are important for fitting the high-precision low-energy scattering data. The F_c, F, $_\delta F$, and $_t F_{ls}$ are short-range functions that represent the finite size of the nucleon charge distributions. They are obtained under the assumption that the nucleon form factors are well represented by a dipole form:

$$G_p^M \quad G_n^M \quad G_D = \left(1 + \frac{q^2}{b^2}\right)^{-2} \qquad (49)$$

$G_E = \mu_p \mu_n$ where $b = 4.27\text{fm}^{-1}$. The functions are given by:

$$F_c(r) = 1 - \left(1 + \frac{11}{6}x + \frac{3}{16}x^2 + \frac{1}{48}x^3\right) e^{-x} \qquad (50a)$$

$$F_\delta(r) = b^3 \left(\frac{1}{} + \frac{1}{}x + \frac{1}{}x^2\right) e^{-x} \qquad (50b)$$

$$\left(16 \quad 16 \quad 48 \right)$$

$$F_t(r)=1-\left(1+x+\frac{1}{2}x^2+\frac{1}{6}x^3+\frac{1}{24}x^4+\frac{1}{44}x^5\right)e^{-x} \qquad (50c)$$

$$F_{\square s}(r)=1-\left(1+x+\frac{1}{2}x^2+\frac{7}{48}x^3+\frac{1}{48}x^4\right)e^{-x} \qquad (50d)$$

with x=br. The derivation of F is given in Ref. [54], while the others are related by: $_c$

$$F_\delta=-\nabla^2\left(\frac{F_c}{r}\right),\ F_t=\left(\frac{F_c}{r}\right)''-\left(\frac{F_c}{r}\right)'/r,\ F_\delta=-\nabla^2\left(\frac{F_c}{r}\right) \qquad (50e)$$

In the limit of point nucleons, $F_c=F_t=F_{\square s}=1$, and $F_\delta=)(4\pi\delta^3 r^{\square}$. The use of F and $_c F_{VP}$ is an approximate method of removing the $1/r$ singularity (the logarithmic singularity remains) which is justified by its short-range and overall smallness of the term. Similarly, the use of F_c^2 and V_{C2} is an approximate method of removing the $1/r^2$ singularity. Because the Sachs nucleon form factors are used, they are no additional magnetic Darwin-Foldy terms [55]. For the np system a Coulomb term attributable to the neutron charge distribution, in addition to the interaction between magnetic moments, are included:

$$\upsilon^{EM}(np)=V_{C1}(np)+V_{MM}(np) \qquad (51)$$

$$F^{np}(r) \text{ where } V_{C1}(np)=\alpha\beta_n \frac{}{r}$$

(51a) where the function F is obtained assuming the neutron electric form factor [55]: $_{np}$

$$^{n} \quad q^2\left(1+\frac{}{}bq^{22}\right)^{-3}$$

(52)

$$G_E=\beta_n$$

here $\beta_n=\left[dG_E^{\,n}/dq^2\right]_{q=0}=0.0189\,fm^2$, the experimentally measured slope [56]. This form factor is checked in a self-consistent calculation of the deuteron structure function q(A^2)used to extract G [57], and find it gives fairly a good fit to the data. This simple form leads to: $^{n}{}_E F_{np}(r)=b^2$

$$\left(15x+15x^2+6x^3+x^4\right)e^{-x}/384 \qquad (53)$$ The magnetic moment interaction is given by:

$$V_{MM}(nn)=-\frac{}{4M\alpha M}\mu_n\mu_p\left[\frac{}{32}F_\delta(r)\sigma_{\square i}.\sigma_{\square j}+\frac{}{}F_t r(_3r)\,S_{ij}\right]$$

$n \quad p$

$$- \overline{2M\alpha_n M_r} \mu_n \overline{F_{ls} r(_3 r)} \left(L \square .S \square + L \square .A \square \right) \qquad (51b)$$

where M_r is the nucleon reduced mass. The term proportional to $A \square = {}^1\!/_2 \left(\sigma \square_i - \sigma \square_j \right)$ is a "class IV" charge-asymmetric force [58], which mixes spin-singlet and spin-triplet states. Its contribution is very small, and it is only included when the magnetic moment scattering amplitude is constructed. Finally, for nn scattering, the Coulomb interaction between the neutron form factors is neglected, so there is only a magnetic moment term: $\upsilon^{EM}(nn) = V_{MM}(nn) =$

$$- 4\alpha M_{n2} \mu_n^2 \left[\left| \right| {}^2\!/_3 F\delta(r) \overline{\sigma \square_i . \sigma \square_j} + \overline{\frac{F_t}{r(_3 r)}} S_{ij} \right] \left| \right| \qquad (54)$$

The charge-dependent structure of the OPE potential is the same as that used in the Nijmegen partial-wave analysis and reads:

$$\upsilon^{\pi}(pp) = f_{pp}^2 \upsilon_{\pi}(m_{\pi^0})$$

$$\upsilon^{\pi}(np) = f_{pp} f_{nn} \upsilon_{\pi}(m_{\pi^0}) + (-1)^{T+1} 2 f_c^2 \upsilon_{\pi}(m_{\pi^{\pm}}) \qquad (55a)$$

$$\upsilon^{\pi}(nn) = f_{nn}^2 \upsilon_{\pi}(m_{\pi^0})$$

^{2}

which $\upsilon_{\pi}(m) = \left| \right| \left(\overline{m m_s} \left| \right| \right) \backslash {}^1\!/_3 mc^2 \left[Y_{\mu}(r) \sigma \square_i . \sigma \square_j + T_{\mu}(r) S_{ij} \right] \qquad (55b)$

$\backslash$

Strictly speaking, the neutron-proton mass difference gives rise to an OPE "class IV" force as well, which again only is explicitly included when the OPE scattering amplitude [59] is constructed. Here, $Y_{\mu}(r)$ and $T_{\mu}(r)$ are the usual Yukawa and tensor functions with the exponential cutoff of the *UrbanaV*$_{14}$ and *ArgonneV*$_{14}$ models:

$$\mu \qquad \overline{\quad} \qquad e_{-\mu r} \left({}^{-cr_2} \right)$$

(56a)

$$Y(r) = \qquad 1 - e$$

$$\mu r$$

$$\mu \qquad \left(\overline{3} \quad \overline{\quad 3 \quad} \right) e^{-\mu r} \left(\quad {}^{-cr_2} \right)_2 \qquad (56b)$$

$$T(r) = \left| \right| 1 + \mu r + (\mu r)^2 \left| \right| \backslash \mu r \; 1 - e$$

$\backslash$ where $\mu = mc/\square$. The scaling m , introduced in Eq. (55b) to make the coupling constant

$_s$ dimensionless, is taken to be the charged-pion mass $)(m_{\pm}$. The Nijmegen partial-wave-

π analysis of NN scattering data below 350 MeV finds very little difference between the coupling constants [60]; so, they are

chosen to be charge-dependent, i.e. $f_{pp} = -f_{nn} = f_c \equiv f$, with recommended value $f^2 = 075.0$. Thus, all charge dependence in Eq. (55) is due simply to the difference in the charged- and neutral-pion masses. The remaining intermediate- and short-range phenomenological part of the potential is expressed, as in the *Argonne*V_{14} model, as a sum of central, L , spin-spin, and quadratic spin-orbit terms (abbreviated as c, ^{2} □2, t, □s , □s2, respectively) in different S, T, and T_z states: $\upsilon_{STR,NN} = \upsilon_{STc,NN}(r) + \upsilon_{ST\square 2,NN}(r)L_2 + \upsilon_{STt,NN}(r)S_{12}$

$$+\upsilon_{ST\square s,NN}(r)L\square.S\square + \upsilon_{ST\square s2,NN}(r)\left(L\square.S\square\right)^2 \qquad (57a)$$

each of these terms, is given in the following general form: $\upsilon_{ST^i} = I_{ST^i,NN}T_\mu^2(r) + \left[P_{ST^i,NN} + \mu r Q_{ST^i}\right.$

$_{.NN} + (\mu r)^2 R_{ST^i,NN}\left.\right]W(r)$ (57b) where $\mu = \frac{1}{3}(m_{\pi_0} + 2m_{\pi_\pm})$, is the average of the pion masses and r(T_μ) is given by Eq. (56b).

Thus, the T_μ^2(r)term has the range of a two-pion-exchange force. The W(r) is a Woods-Saxon function, which provides the short-range core:

$$W(r) = \left[1 + e^{(r-r_0)/a}\right]^{-1} \qquad (58)$$

The four sets of constants $I_{ST^i,NN}$, $P_{ST^i,NN}$, $Q_{ST^i,NN}$, and $R_{ST^i,NN}$ are parameters to be fit to data. However, a regularization condition at the origin which reduces the number of free parameters by one for each $\upsilon_{ST^i,NN}$, also, imposes.

The following expressions are required:

$$\upsilon_{ST^i\ ,NN}(r=0) = 0 \qquad (59a)$$

$$\left.\frac{\partial \upsilon_{STi\neq t,NN}}{\partial r}\right|_{r=0} = 0 \qquad (59b)$$

Since the tensor part of the OPE potential already vanish at r=0, the first condition is satisfied by setting $P_{ST^t,NN} = 0$. The second condition is equivalent to fitting, for i≠t :

$$Q_{ST^i\ ,NN} = -\frac{}{\mu W1(0)}\left[\left|P_{ST^i,NN}\frac{}{}\frac{\partial \upsilon_{ST}^{\pi}}{\partial r} + \delta_{ic}\frac{\partial W}{\partial r}\right]\right|_{r=0} \qquad (59c)$$

where only the derivation of the spin-spin part of the OPE potential have to be evaluated. The projecting of this potential into operator format, the value of the fundamental constants, and other complete treatments about the potential, is found in the related paper [52].

(4.11) Bonn Group Potentials

In the first version, in 1987, Bonn group presented a comprehensive field theoretical meson-exchange model for NN interaction below pion products threshold, consisting of all diagrams

that they believed to be important [61]. The Full-Bonn potential is an NN momentum-space potential. Next to π, ω, and δ exchanges, the model also contains an explicit determination of the TPE contribution, including ρ exchange and virtual isobar excitation. In addition, higher-order diagrams involving heavy-meson exchanges are included, specially the combination of π, ρ, which proves to be crucial for a quantitative description of the low angular momentum phase shifts of NN scattering. This model yields a definite prediction of the meson-nucleon (-isobar) vertex parameters (coupling constants and cutoff parameters of the vertex form factors). The model provides a sound basis for addressing several important issues in nuclear physics, such as three-body forces, meson-exchange currents, charge symmetry, independence violations, and relativistic effects of the nuclear medium on the NN force in the nuclear many-body problem. The coordinate-space version is obtained from a simple parameterization of the Full model by six OBE terms (three pairs of pseudoscalar, vector, and scalar mesons, respectively). The potentials are regularized at the origin by means of dipole-form-factor functions. As a whole, it is determined that the FullBonn potential gives a good description of the NN scattering data. Its final version was published in 1989. The short-range part of this model was defined by attaching phenomenological form factors to the momentum-space Feynman diagrams and regularizing the high-momentum part of the scattering amplitude with cutoffs. The cutoff masses were adjusted to fit experimental data. Among numerous different versions of the Bonn potential, the best ones are the Full-Bonn potential [61], the Bonn-B OBEP [62], and Bonn-CD [63, 64], where the last one is the best of all. The difference of two first ones lies mainly in the fact that the Full model includes correlated two-pion and πρ contributions with intermediate delta (Δ) isobars, while the Bonn-B is a "classical" one-boson-exchange model using a fictitious sigma (σ) meson to represent two-pion-exchange. In contrast to the Full model, the Bonn-B potential is energy-independent which simplifies applications in nuclear structure and nucleon-nucleus scattering calculations. Despite its simplicity, the Bonn-B potential gives results almost identical to those found by using the Full model. In summary, the Bonn-B potential is a simple meson-theoretical model that gives a good description of the scattering data of that time. However, in a work performed in 1993 [65] in order to compare some of the potential forms with pp scattering data below 350 MeV, it was demonstrated that the adjusted coordinate-space versions [62], Bonn A- and Bonn-B models, give a very poor description of the scattering data ($\chi^2 / N_{data} > 8$ in the 2-350 MeV energy range). However, the CD-Bonn potential is a charge-dependent NN potential that fits the world pp data below 350 MeV available in the year of 2000 with a $\chi^2 / N_{data} = 01.1$, for 2932 data and the corresponding np data with $\chi^2 / N_{data} = 02.1$, for 3058 data. This reproduction of the NN data is more accurate than by any phase-shift analysis and any other NN potential (in its author opinion, of course!). The charge-dependence of the present potential (that has been dubbed "CD-Bonn") is based upon the predictions by the Bonn Full model for charge-symmetry and charge-independence breaking in all partial waves with $J \leq 4$. The potential is represented in terms of the covariant Feynman amplitudes for non-boson exchange that are non-local. Therefore, the off-shell behavior of the CD-Bonn potential differs in characteristic and leads to larger binding energies in nuclear few- and many-body systems, where underbinding is a persistent problem. The model, besidesπ, includes the ρ(769), and ω)783(vector mesons and also two scalarisoscalar δ bosons, using covariant Feynman

amplitudes for their exchanges. The comprehensive discussion about these potentials is found in the mentioned references above.

(4.12) Hamburg Group Potential

Since in the Bonn-B model, the scattering amplitudes are obtained from the mesonbaryon lagrangian in a clear and comprehensive fashion, this model is used as a base in the construction of the one-solitary-boson-exchange potential (OSBEP). In fact, the Hamburg's group potential revamps the boson exchange picture seeking a procedure that reduces markedly the numbers of parameters of the conventional boson exchange models required for them to provide quality fit to scattering data. This model (OSBEP) has the very desirable feature that it does not require (arbitrary) cutoffs, as do the conventional ones. Besides, this OSBEP model casts the nucleon-nucleon- and pion-nucleon- potential into one shape frame; the model also gives a good quantitative description of the experimental data. Refs. [66, 67] discuss on this potential in detail.

(4.13) Moscow Type NN Potentials, etc.

In the related paper [68], a detailed description of Moscow-type (M-type) potential models for the NN interaction is given. The microscopic foundation of these models, which appear because of the composite quark structure of nucleons, is discussed. M-type models are shown to arise naturally in a coupled channel approach when compound or bag-like six-quark states, strongly coupled to the NN-channel, are eliminated from the complete multi-quark wave function. The role of the deep lying bound states that appear in these models is elucidated. By introducing additional conditions of orthogonality to these compound sixquark states, a continuous series of almost on-shell equivalent non-local interaction models, characterized by a strong reduction or full absence of a local repulsive core (M-type models) is generated. The predictions of these interaction models for 3N systems are analyzed in detail. It is shown that M-type models give, under certain conditions, a stronger binding of the 3N system than the original phase-equivalent model with the new versions of the Moscow NN potential describing also the higher even partial waves is presented. Large deviations from conventional NN force models are found for the momentum distribution in the high momentum region. In particular, the coulomb displacement energy for nuclei

$^3He - {}^3H$ displays a promising agreement with experiment when the H^3 binding energy is extrapolated to the experimental value. A new mechanism for intermediate-and short-range NN interaction is given by these group members [69].

Besides the NN potential forms mentioned above, other NN interaction forms also exist. For instance, almost all of the potential models are mentioned in Ref. [70]. **(4.14) Imaginary Potentials**

Many imaginary NN potentials are presented. In a work [71], the NN potentials of Paris, Nijmegen, Argonne, and those derived by quantum inversion, which describe the NN interaction for T-lab below 300 MeV, are extended in their range of application as NN optical models. Extensions are made in configuration-space using complex separable potentials definable with a wide range of form factor options including those of boundary condition models. The new phase shift analyses from 300 MeV to 3 GeV to determine these extensions are used. The imaginary parts of the optical model interactions account for loss of flux into direct or resonant production processes. The optical potential approach is of particular value as it permits one to visualize fusion, and subsequent fission of nucleus when T-lab above 2 GeV. They do so by calculating the scattering wave functions to specify the energy and radial dependences of flux losses and of probability distributions. Furthermore, half-off the energy shell T-matrices are presented as they readily deduced with this approach. Such matrices are required for studies of few- and many-body nuclear reactions. Details are in Ref. [71].

5. A Comparison of Some NN Potential shapes

(5.1) Introduction

As already mentioned in the section three, various potential models have been given for the description of nucleon-nucleon interaction. The models based on Quantum Chromo Dynamics (QCD), Effective Field Theory (EFT), Chiral Perturbation Theory (CHPT), Boson Exchange (BE), and pure phenomenological are outstanding ones. A definite thing is that the models based on QCD and EFT need more quantitative improvements; these models describe characteristic phenomena that are observed in Nucleon-Nucleon, Pion-Nucleon, and PionPion scattering quite well but quantitatively they fail. Common features of "QCD-inspired" models that detract from their appeal are cumbersome mathematics, large numbers of parameters, and a limitation in applications essentially to very low energies. On the other hand, the boson-exchange models have a further intimacy with the fact of NN interaction so that for example, in the OBEP models to each set of mesons, at one part of the interaction, a role is given. e.g., in general, when six non-strange bosons mentioned previously, i.e., the pseudoscalar mesons π and η, the vector mesons ρ and ω, and two scalar boson δ and σ, where the first particle in each group is isovector while the second is isoscalar, with masses below 1GeV, are taken into account; the pion (π) provides the tensor force, which is reduced at short range by ρ meson. The ω, creates the spin-orbit force and the short-range repulsion, and the σ is responsible for the intermediate-range attraction. Thus, it is easy to understand why a model which includes the above four mesons can reproduce the major properties of the nuclear force (see, Ref. [30], Secs. 3 and 4). In this case, besides the above meson exchanges, other different meson exchanges are also considered and the strength for every kind of meson exchanges (e.g., multi-meson exchanges) that are not considered, is delivered as a parameter to be determined by fitting to the NN scattering data. On the other hand, about the phenomenological NN potential models, the most important feature of those is their simplicity; general form of potential allowed by symmetries like rotation, translation, isospin, and… is considered, in this model; in these potentials, intermediate- and short-range parts are determined wholly in a phenomenological way and for long-range part, one pion exchange potential is often used. There are however some undesirable problems yet, e.g., in a phenomenological potential model that uses the Yukawa type functions $\varphi(r) = g/4\pi r\, exp(-\frac{mc}{\hbar} r)$ (and for other function types as well), the masses at the exponent and the other similar free parameters, are obtained by fitting to the NN scattering data. These cases (as in the case of boson-exchange potentials where some parameters having physical meaning have been put free to be determined by means of fitting to data) are weakness because the nuclear force in principle should not be dependent to these external restrictions so much; although these problems should not decrease from the successes obtained by these potentials. In spite of the problems we have already mentioned some of them; the successes of these models are yet noticeable and give satisfactory results in the many of the nuclear structure calculations. In Sec. (5.2), we shall briefly review the methods to compare different potentials, and finally give a conclusion about NN interaction.

(5.2) Comparison of the Various Forms of Two-Nucleon Potential

The quality measurement of the various NN potentials is possible through several methods. Giving satisfactory results in the nuclear structure calculations, and the deuteron

parameters (such as, D-state probability, the ratio of D-wave to S-wave, quadratic magnetic moment, electric quadruple moment, and binding energy) are two outstanding ways. It is of course necessary to mention that some of the potential forms use these empiric parameters in order to fit. Giving phase shifts in different channels and comparing those with empiric values, is another method of potential quality measurement (PQM), specially the χ^2 associated with the fitting of the experimental NN data by means of potential has been considered as a desirable parameter for the potential quality measurement (PQM) as is considered in the description of different potential forms. In the case of using the χ^2 for the potential quality measurement (PQM), however, some discussions are exist [31]; For instance, a considerable point is that the χ^2 is not a magic number, since its relevance with regard to the "quality" of a potential is limited. Consider, for example, a model based on little theory, but with many parameters; this model will easily fit the data well and produce a very low χ^2 (e.g., $\chi^2/datum \approx 1$). However, we will not learn much basic physics from this. On the other hand, think of a model with a solid theoretic basis and (therefore) very few parameters (with each parameter having a physical meaning); here the comparison with the experimental data may teach us some real physics. In such as case, a $\chi^2/datum$ of 2 or 3 may be excellent. Thus, the χ^2 represents only one aspect among several others that needs to be considered simultaneously when judging the quality of a NN potential. Other aspects of equal importance are the theoretical basis of a potential model and (closely related) its off-shell behavior (that can, of course, not be tested by calculating the χ^2 with regard to the on-shell NN data). This latter aspect is important, particularly, for the application of a NN potential to nuclear structure. In fact, one can demonstrate that the variation of the $\chi^2/datum$ between 1 and 6 affects nuclear structure results only in a negligible way, while off-shell differences are of substantial influence. Notice also, that the χ^2 sometimes blows up small differences between theory and experiment in a misleading way. This is so, in particular, when the experimental error is very small (a good example for this is the pp data below 3 MeV). In such cases, the χ^2 is more a reflection of the experimental precision than of the quality of the theory.

In summary, overestimating the importance of the χ^2 may miss the physics. Another discussion is that if one can consider the χ^2, it is insufficient to consider it for the pp data only. If one calculates a χ^2, one should do it by all means properly. The most important rule here is that a pp potential must only be confronted with pp data, while a np potential must be confronted with np data. Further and more complete on these problems is found in Ref. [72].

According to above discussions, we, here, try to compare (some) potentials in a somewhat substantial way, i.e., by considering their structures directly. Before going into this method, we mention one case of the potential comparison by means of different period data that have been performed by several groups.

In a work performed in 1993, some of the potential forms (shapes) i.e., HamadaJohnston potential [21], Reid soft-core potential [23], super-soft-core potential [27], Funabashi potential [29], Nijm78 potential [36], parameterized Paris potential [43], $Argonne V_{14}$ potential [51], coordinate-space Bonn potential [61], and Bonn89 potential were compared with pp scattering data below 350 MeV. Of the older models only the Reid68, Nijm78, and Paris80 models give satisfactory results when confronted with the pp data. The new Bonn89 model, an adjustment of the Full-Bonn potential to fit explicitly the pp data, is of a similar quality as the Nijm78 and Paris80 potentials in the 2-350 MeV energy range. If the very low-energy data (0-2 MeV) include only the Nijm78 and Bonn89 potentials still give a

reasonable description of the data. The other models all give a large to very large contribution to χ^2 in this low-energy region. The reason is that the pp $^1S_0$ phase shift at $T_{Lab} = 382.54 KeV$ is very accurately known. So a small deviation for the $^1S_0$ prediction from one of these potential models will give rise to an enormous contribution to χ^2. However, this contribution should not be too large, since most potential models claim to give a good description of the scattering length and effective range parameters. Furthermore, the fact that some of the models give a rather poor description of the pp data is not only due to an incorrect $^1S_0$ phase shift. As an example, consider the $Argonne V_{14}$ potential. In the 0-350 MeV energy range the $Argonne V_{14}$ model gives $\chi^2 / N_{data} = 7.1$. When we replace the $Argonne V_{14}$ $^1S_0$ phase shifts by multi-energy values (which roughly corresponds to having a model with "perfect" $^1S_0$ phase shift), the quality of the model improves considerably. However, the resulting $\chi^2 / N_{data} \approx 4$ is still rather large. This demonstrates that the other phase shifts are not too good either. An important conclusion which can be drawn from the potential comparison with the pp scattering data discussed in Ref. [66] is that only the potential models which were explicitly fitted to the pp data (Nijm78, Paris80, Bonn89) give a reasonable description of these data. Here, it has to keep in mind that the Nijm78 and Paris80 models were fitted to the 1969 Livermore database [38]. However, the database used in Ref. [55], contains a large number of new and more accurate data, which are still described rather well by these two models. The Bonn89 potential was fitted to a much more recent database, not too different from the database in Ref. [65]. Apparently, a good fit to the pp data dose not automatically guarantee a good fit to the np data. One of the reasons is that the np data are less accurate than the pp data, so the constraints on the np phase shifts are not so large. In addition, the difference between the pp and np $^1S_0$ phase shifts should be included explicitly.

The Nijm93, NijmI, NijmII, and Reid93 potentials give a χ^2 / N_{data} 1.08, 1.03, 103, and 1.03, respectively. For partial wave analysis (PWA), a related value is 0.99. As already mentioned, the $Argonne V_{18}$ potential was fitted to both the pp and np scattering data of Nijmegen group [30], and low nn energy scattering data as well as deuteron binding energy; and by having 40 adjustable parameters gives $\chi^2 / N_{data} = 09.1$ for 4301 pp and np data in the 0-350 MeV energy range. The CD-Bonn potential, also, fits the pp scattering data below 350 MeV available in 2000 with $\chi^2 / N_{data} = 1.02$ for 3058 data. Therefore, for the approach in which χ^2 is considered for the potential quality measurement (PQM), one can, in general, present the following issues: In the 1990's a focus has been on the quantitative aspect of NN potentials. Even the best NN models of the 1980's (Paris and Full-Bonn models) fit the NN data typically with a $\chi^2 / N_{datum} \approx 2$ or more. This is still substantially above the perfect $\chi^2 / N_{datum} \approx 1$. To put microscopic nuclear structure theory to a reliable test, one needs a perfect NN potential such that discrepancies in the predictions cannot be blamed on a bad fit of the NN data. Based upon the Nijmegen analysis and the (pruned) Nijmegen database, new charge-dependent NN potentials were constructed in the early/mid 1990's. The most noticeable involved groups and the names of their new creations are, in chronological order: (1) Nijmegen group [37]: NijmI, NijmII, and Reid93 potentials. (2) Argonne group [52]: AV_{18} potential. (3) Bonn group [63, 64]: CD-Bonn potential. All these potentials have in common that they use about 45 parameters and fit the 1992 Nijmegen database with a $\chi^2 / N_{datum} \approx 1$. However, because from 1992 on, the pp database has substantially been expanded and therefore, for the current database the χ^2 / N_{datum} produced by some potentials is not so perfect anymore [3]. Nevertheless, the above potentials are almost best present potentials.

(5.3) Structural Comparison of the Potentials Reduced into Reid Potential

Because of the existence of a large number of potentials, we here consider some potential forms, i.e., Ried68 potential and an extended version of it to higher orders by B. D. Day that we name Reid68-Day potential, Reid93 potential, *Urbana*V_{14} potential, *Argonne*V_{18} potential, and Nijm93, NijmI, NijmII potentials. In another moment, we shall make the above set more complete than now. Since, Reid used the central potential for singlet- and triplet- uncoupled states, and for triplet coupled states a potential having the central, tensor, and the first order spin-orbit was used, i.e.:

$$V = V_C(r) + V_T(r)S_{12} + V_{LS}(r)L\square.S\square \qquad (22)$$

Thus, we reduce the mentioned potentials above for all uncoupled and coupled states to the Reid potential form. In other words, because for full Reid potential, three terms i.e. central, tensor, and spin-orbit are considered therefore, for above potentials, after our reduction plan, only these three terms remain. The most important reason to doing this a work is that besides the fact that not only the main terms in a potential are these three terms but also with having a similar operator shape (form) for potentials, one can compare potentials structurally as well.

(5.3.1) The Reduction of UrbanaV$_{14}$ Potential into Reid Potential: In the UV_{14} model [45], the two-nucleon interaction is as follows:

$$V_{ij} = \sum_{p=1,14} \left(\upsilon_\pi^R(r_{ij}) + \upsilon_I^p(r_{ij}) + \upsilon_S^p(r_{ij})\right) O_{ij}^p \qquad (43)$$

for long-range part, it reads:

$$\upsilon_\pi = \upsilon_\pi^{\sigma\tau}(r)(\sigma\square_1.\sigma\square_2)(\tau\square_1.\tau\square_2) + \upsilon_\pi^{t\tau}(r)S_{12}(\tau\square_1.\tau\square_2) \qquad (60)$$

and for intermediate-range part, we have:

$$\upsilon_I = T_{\pi 2}(r)(I_c + I_\sigma(\sigma\square_1.\sigma\square_2) + I_\tau(\tau\square_1.\tau\square_2) + I_{\sigma\tau}(\sigma\square_1.\sigma\square_2)(\tau\square_1.\tau\square_2)$$

$$+ I_t S_{12} + I_{t\tau} S_{12}).().().(\tau\square_1\tau\square_2 + I_q L_2 + I_{q\sigma} L_2\sigma\square_1\sigma\square_2 + I_{q\tau} L_2\tau\square_1\tau\square_2$$

$$+ I^{q\sigma\tau} L^2)).().().().(.(\sigma\square_1\sigma\square_2\tau\square_1\tau\square_2 + I^{bb} L\square S\square^2 + I^{bb\tau} L\square S\square^2\tau\square_1\tau\square_2$$

(61) as well as for the short-range part, it becomes: $\upsilon_S = W(r)(S_c + S_\sigma(\sigma\square_1.\sigma\square_2) + S_\tau(\tau\square_1.\tau\square_2) + S_{\sigma\tau}(\sigma\square_1.\sigma\square_2)(\tau\square_1.\tau\square_2)$

$$+ S_b(L.S) + S_{b\tau}(L.S)(\tau\square_1.\tau\square_2) + S_q L_2 + S_{q\sigma} L_2(\sigma\square_1.\sigma\square_2)$$

$$+ S_{q\tau} L_2)).().().().(.().(\tau\square_1\tau\square_2 + I_{q\sigma\tau} L_2\sigma\square_1\sigma\square_2\tau\square_1\tau\square_2 + I_{bb} L\square S\square_2 + I_{bb\tau} L\square S\square_2\tau\square_1\tau\square_2$$

$$+ W')).)(.().()((r S'^b L\square S\square + S'^{b\tau} L\square S\square\tau\square_1\tau\square_2 \qquad (62)$$

which in the above relations both I^p, S^p, S'^p and $T_\pi(r)$, $W(r)$, $W'(r)$ are the functions of r

which are given in the Eq. (44) and (46b) respectively. In our reduction plan, we now compute the expectation values of all operators at that state and therefore, as in the Reid potential, we shall finally have only a function of r, for uncoupled states. Required expectation values are given at Sec. (3.3.2). Therefore, for an uncoupled state, e.g., for ${}^3P_0$ state, one, after a little computation, finally obtains:

$$V({}^3P_0) = 2694.69W(r) + 4400W'(r) - 3.6T_\pi^2(r) + \upsilon_\pi^{\sigma\tau}(r) - 4\upsilon_\pi^{t\tau}(r) \quad (63)$$

for a coupled state, e.g., for ${}^3S_1 - {}^3D_1$ state, in the end, one can obtain as well:

$$V({}^3S_1 - {}^3D_1) = (2399.99W(r) - 6.8008T_\pi^2(r) - 2\upsilon_\pi^{\sigma\tau}(r)) + (0.75T_\pi^2(r) - 3\upsilon_\pi^{t\tau}(r))S_{12} + (80W(r))L\square.S\square \quad (64)$$

It is necessary to mention that in our reduction plan, for coupled states, $\square = j - 1$ is considered.

(5.3.2) The Reduction of ArgonneV_{18} Potential into Reid Potential: In this case, by considering the operator forms (shapes) of the potential [52], which 14 operators (from 18 operators) of it are the same as those of *Urbana*V_{14} potential, the reduction performs as in the *Urbana*V_{14} case. However, because of the presence of four new operators (three charge-dependence operators, and one charge asymmetry operator), together with a full electromagnetic interaction, a little more lengthy computation is required, that we do not express here its detail.

(5.3.3) The Reduction of Nijm93, NijmI, and NijmII Potentials into Reid Potential: These potentials [37] have already been discussed in the Sec. (4.7). The potentials, in configuration space, have a structure as follows:

$$V = V_C(r) + V_{SS}(r)(\sigma\square_1.\sigma\square_2) + V_T(r)S_{12} + V_{LS}(r)L\square.(\sigma\square_1 + \sigma\square_2)/2 + V_{LSA}(r)L.(\sigma_1 - \sigma_2)2 + V_{Q12}(r)\left[(\sigma_1.L\square)(\sigma_2 - .L\square) + (\sigma_3.L\square)(\sigma_1.L\square)\right]2 \quad (65)\ \square$$

The Nijm93 and NijmI potentials have a little non-locality in their central parts, i.e.:

$$V_C(r) = V_C(r) - \frac{1}{2M_{red}}[\nabla^2\phi(r) + \phi(r)\nabla^2] \quad (66)$$

However, in the NijmII potential, $\phi(r) \equiv 0$. As previously discussed in the Sec. (4.7), the antisymmetric spin-orbit part, in principle, does not use in these models. On the other hand:

$$Q_{12} = \left[(L\square.S\square)^2 - \delta_{LJ}L^2\right] \quad (18)$$

Thus, in our reduction plan, by considering the case that for the Nijm93 and NijmI non-local potentials we must add, for uncoupled states, the expectation value of the second term in Eq. (66); therefore, from Eq. (65) we have:

$$V = V_C(r) + V_{SS}(r)(\sigma\square_1.\sigma\square_2) + V_T(r)\,S_{12} + V_{LS}(r)\,L\square.S\square$$

$$V_{Q12}\left\langle (r)(L\square.S\square)^{2}-\delta_{LJ}L^{2}-\right\langle \qquad 1$$

$$[\nabla^{2}\phi(r)+\phi(r)\nabla^{2}] \qquad \left\langle (67)\right\rangle$$

$$+ \qquad\qquad \left\langle \right\rangle$$

$$2M_{red}$$

For singlet-coupled states, as already discussed, the tensor and spin-orbit terms become zero, and in the uncoupled states except ${}^{3}P_{0}$ state, $\langle \delta_{LJ}L^{2}$ is not zero. On the other hand, one can easily compute $\nabla^{2}\phi(r)$ by having $\phi(r)$. Also, in order to compute $\langle \phi(r)\nabla^{2}\rangle$, by using the Laplacian in the spherical coordinate, at a state with a definite angular momentum, we have:

$$\left\langle \right\rangle^{2}(r)\square L_{2}r^{2}{}^{2}=-\phi(r)\square(\square_{r}+1) \qquad (68)$$

$$\phi(r)\nabla=-\phi$$

The reduction to three terms of Eq. (22) performs in a same way; since in all coupled states, $L\neq J$, therefore $L^{2}\delta_{LJ}$ is zero, and in the end (in our scheme):

$$V_{Central}=V_{C}(r)+V_{SS}(r)\,(\sigma\square_{1}.\sigma\square_{2})-\frac{1}{2M_{red}}[\nabla^{2}\phi(r)+\phi(r)\nabla^{2}] \qquad (69a)$$

$$V_{Tensor}=V_{T}(r) \qquad (69b)$$

$$V_{\text{Spin-Orbit}}=V_{LS}(r)+V_{Q12}(r)\langle L\square.S\square \qquad (69c)$$

One can obtain the expectation values of Eq. (67) and (69) as in the Sec. (3.3.2).

(5.3.4) Results and Discussion: In table 1. some of the considered states together with their quantum numbers are given. In our reduction plan, three kinds of potential, i.e. central (for all states), tensor, and spin-orbit, which the last two kinds are only present in the coupled states, exist. In the charge-independent Reid68 potential, states up to $J\leq 2$ are only included, and for $J>2$ states, only in the tensor potential, OPEP is used. B. D. Day extended the Reid68 potential up to $J\leq 5$ states, and at this case for $J>5$ states, he puts the tensor potential of the OPEP type and for spin-orbit from $J\geq 5$ on, he sets a zero value. The charge-dependence Reid93 potential has the states up to J=9 in the central and tensor parts, and for the spin-orbit potentials in the states from $J\geq 5$ on, he sets a zero value as was done by Day while he extended the Reid68 potential to higher states. The charge-dependent Nijm93, NijmI, and NijmII potentials have the same states as Reid93 potential as well. The charge-independent *Urbana*V_{14} potential has states up to F (J=3) and the charge-dependent *Argonne*V_{18} potential has all three kind of potentials up to higher states.

The Reid93 and *Argonne*V_{18} potentials do not use meson exchange for intermediate and short ranges; instead, a phenomenological parameterization is chosen. The *Argonne*V_{18} uses local functions of Woods-Saxon type, while Reid93 applies local Yukawas of multiples of pion mass, similar to the original Reid68 potential. In the *Urbana*V_{14} potential, for the intermediate- and short- range parts, a phenomenological parameterization is also chosen, and the local functions of the usual Yukawa type together with exponential cutoff are used which the cutoff parameter is determined by fitting to data. At the short-range part, the Woods-Saxon potentials are used.

At very short distances, the potentials are regularized by exponential (AV_{18} , Nijm93, NijmI, NijmII), or by dipole (Reid93) form factors (which are all local functions). The models Nijm93, NijmI, and NijmII are based upon the Nijm78 potential, which is constructed from approximate OBE amplitudes. Whereas the NijmII uses the totally local approximations for all OBE contributions, the NijmI keeps some non-local terms in the central force component (but the Nijm93 and NijmI tensor forces are totally local). Non-localities in the central force have only a very moderate impact on nuclear structure as compared to non-localities in the tensor force. Thus, if for some reason one wants to keep only some of the original non-localities in the nuclear force and not all of them, then it would be more important to keep the tensor force non-localities. According to discussions up to now, it is determined that the form of the Reid68 and Reid93 potentials are similar and for each of two sets of UV_{14} and AV_{18} potentials, and also Nijm93, NijmI, NijmII potentials, as well.

In Figs. 3, 4, and 5, the central, tensor, and spin-orbit potentials of the various potential models reduced to Reid potential are given for np states from J=0 up to J=9. In the case of the charge-independent potentials, we have only set a present potential in a special case. Although, phase shifts predictions and performed calculations by these potentials give fairly similar results but the potentials are largely different. At the first glance to figures, a close similarity of Reid68 potential to Reid93 potential, and UV_{14} potential to AV_{18} potential, as well as Nijm93, NijmI, NijmII potentials to each other, is obvious and by taking into account already discussion about their structural similarities, is of course reasonable. The weakness (looseness) of a given expansion from Reid68 potential by Day is obvious from figures, since the Day expansion of Reid68 potential was to give exclusively satisfactory results in the nuclear calculation and not based on physical basis. The softness' degree of the potentials is obvious from Figs. as well. The dependency to the even or odd of two-nucleon relative angular momentum that is a representative for spatial exchange is also clear from figures. e.g., at $^1D_2$ channel with an even L, and at $^1F^1$ channel with an odd L, one can easily see, from Fig. 3, which Reid68, Reid93 potentials have a tendency to oppose from each other and so for three Nijmegen potentials; that is, in these potential forms, spatial exchange is strong. For tensor and spin-orbit potentials in Figs. 4 and 5, one can easily see that for each of states with either an even or an odd J, a special procedure is dominant, and present differences are discussable from different point of views. In Figs. 6, 7, and 8, three groups of similar potentials, for the np states from J=0 up to J=2, are compared. In Fig. 6, Reid potentials (Reid68-Day, Reid93) are pictured for some states. In general, the differences of these two potentials have been returned to the discussed differences in the Sec. (4.7). The presence of a softer core in the Reid93 potential is obvious, also low differences in Fig. 7, are expectable on account of the low differences in the structure of UV_{14} and AV_{18} potentials and also for three Nijmegen potentials in Fig. 8. The charge-dependence of the charge-dependent potentials is also showed, for $^1S_0$ central potential, and the tensor potential of

---

$^1P_2 - {}^3F_3$ state, as well as the spin-orbit potential of $^3P_2$ state, in Fig. 9. In Fig. 10, the dependence on orbital angular momentum for $^3S_1$, $^3D_1$, $^3P_2$, and $^3F_2$ states in the case of np system, are pictured which demonstrate an explicit dependence on L, or in other words, the presence of spatial exchanges in these potentials,… .

(5.4) Conclusion and Comment

In the recent decades, many NN potentials have been represented, and their precision and quality were investigated from various methods as well, which the most important method is giving satisfactory results in the nuclear structure calculations. The determination of χ^2/N_{data} is another customary method that, as already discussed, has own difficulties. Based upon these two scales, several high precision charge-dependent NN potentials are given that some of them have already been mentioned in the Sec. (5.2).

A main conclusion that one can deduce from the comparison done here is that a definite and fixed form for NN potential is still a very crucial challenge, because if we have the different shapes for nuclear force, then the nuclear force will obviously become meaningless. A definite thing is that the quantitative similarities are present among these potentials, however, at the same time, the quantitative differences are also present. Generally speaking, one can attribute the quantitative differences of potentials to the theoretical and structural differences mentioned above (e.g., the Yukawa functions, Woods-Saxon functions, form factors in order to regularize a potential at origin, and in general, the functions used in the various parts of potential forms). These differences may be arisen from the approximation and the failures of our knowledge from nuclear force. It is therefore seems that these models in which many approximations (such as, the selection of the special forms for potentials, fitting to data, and …) have been used, are only a temporary way for solution of NN interaction problem. The efforts for finding a fundamental theory of this interaction (which in the public opinion, in spite of the present problems, is QCD) are of course in progress as before. Nevertheless, while these difficulties appear to be important, however, they are not so big that they lead to serious difficulties in their applications into nuclear structure problems. The people who use these potential into their calculations, considering our comparison from some potential forms, may find satisfactory reasons for the present discrepancies in our results. In order to depict figures, Harvard Graphics 98 is used. For computer programs (related computer codes), and probably other related questions, one can also contact with me through electronic address: naghdi.m@gmail.com.

Table 1. *Two nucleon states from J=0 up to J=9 and potential types in our reduction plan; for other higher states, the process is similar, with the J=5 states on named by Latin letters H, I, K, L, M, N, and so on.*

Potential type (state)	*Central*	*Tensor and Spin-Orbit*
$J=0, S=0, T=1, L=0$	$^1S0(pp,np,nn)$	-
$J=0, S=1, T=1, L=1$	$^3P0(pp,np,nn)$	-
$J=1, S=0, T=0, L=1$	$^1P1(np)$	–
$J=1, S=1, T=1, L=1$	$^3P1(pp,np,nn)$	–
$J=1, S=1, T=0, L=0, L=2$	$^3S1-^3D1(np)$	$^3S1-^3D1(np)$
$J=2, S=0, T=1, L=2$	$^1D2(pp,np,nn)$	–
$J=2, S=1, T=0, L=2$	$^3D2(np)$	–
$J=2, S=1, T=1, L=1, L=3$	$^3P2-^3F2(pp,np,nn)$	$^3P2-^3F2(pp,np,nn)$
$J=3, S=0, T=0, L=3$	$^1F3(np)$	–
$J=3, S=1, T=1, L=3$	$^3F3(pp,np,nn)$	–
$J=3, S=1, T=0, L=2, L=4$		

	${}^3D3-{}^3G3(np)$	${}^3D3-{}^3G3(np)$
$J=4, S=0, T=1, L=4$	${}^1G4(pp,np,nn)$	–
$J=4, S=1, T=0, L=4$	${}^3G4(np)$	–
$J=4, S=1, T=1, L=3, L=5$	${}^3F4-{}^3H4(pp,np,nn)$	${}^3F4-{}^3H4(pp,np,nn)$

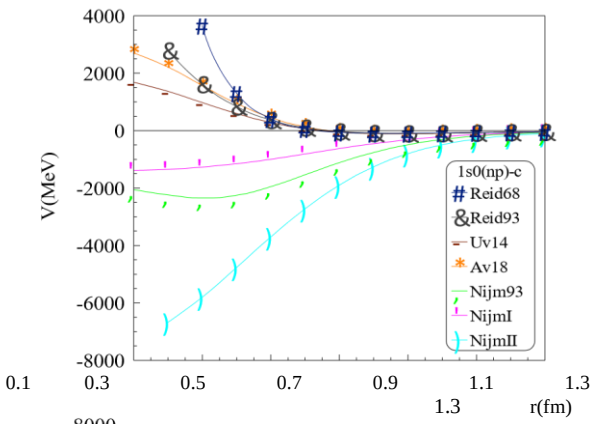
1s0(np)-c
Reid68
Reid93
Uv14
Av18
Nijm93
NijmI
NijmII
V(MeV)
r(fm)

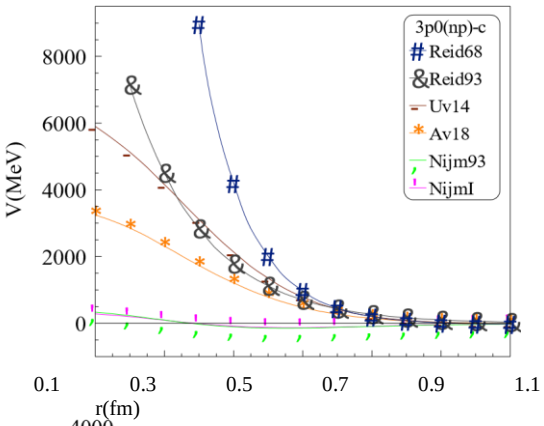
3p0(np)-c
Reid68
Reid93
Uv14
Av18
Nijm93
NijmI
V(MeV)
r(fm)

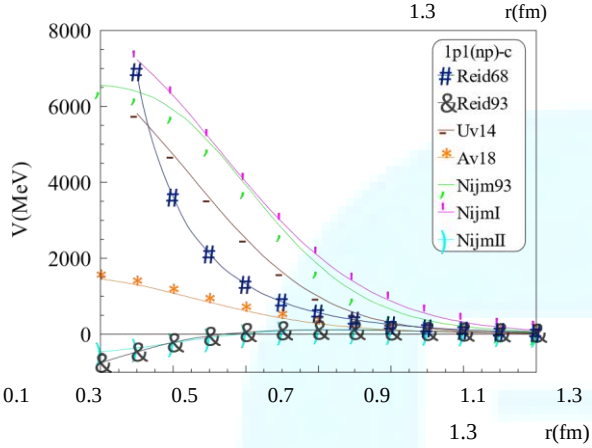
1p1(np)-c
Reid68
Reid93
Uv14
Av18
Nijm93
NijmI
NijmII
V(MeV)
r(fm)

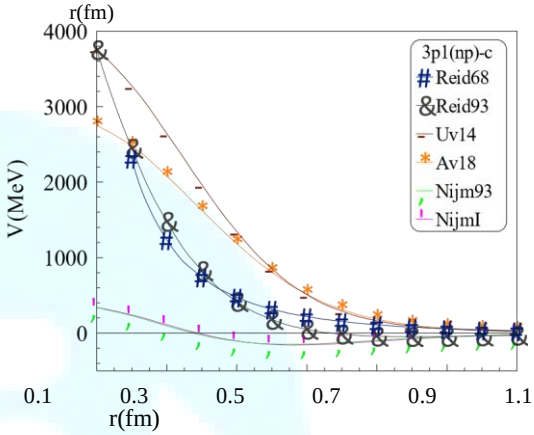
3p1(np)-c
Reid68
Reid93
Uv14
Av18
Nijm93
NijmI
V(MeV)
r(fm)

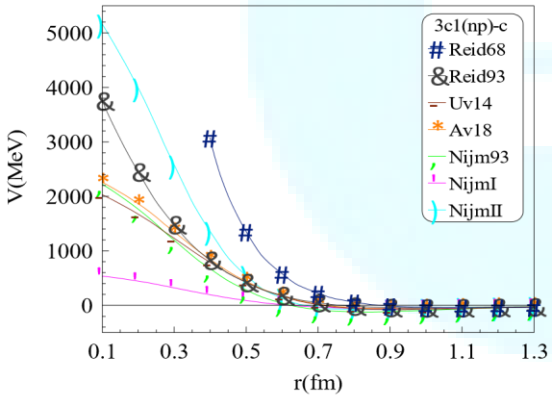
3c1(np)-c
Reid68
Reid93
Uv14
Av18
Nijm93
NijmI
NijmII
V(MeV)
r(fm)

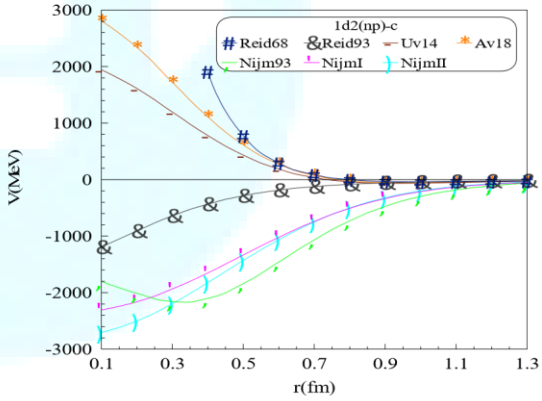
1d2(np)-c
Reid68
Reid93
Uv14
Av18
Nijm93
NijmI
NijmII
V(MeV)
r(fm)

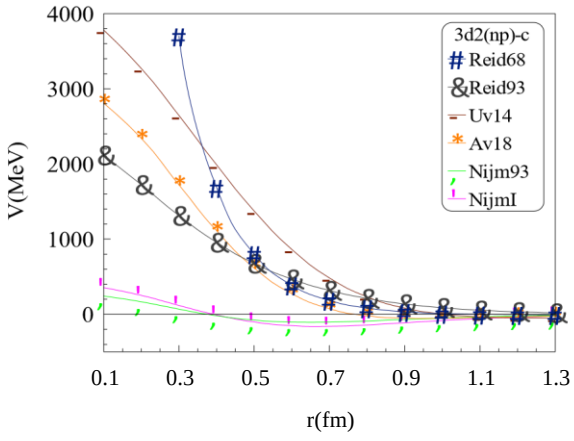
3d2(np)-c
Reid68
Reid93
Uv14
Av18
Nijm93
NijmI
V(MeV)
r(fm)

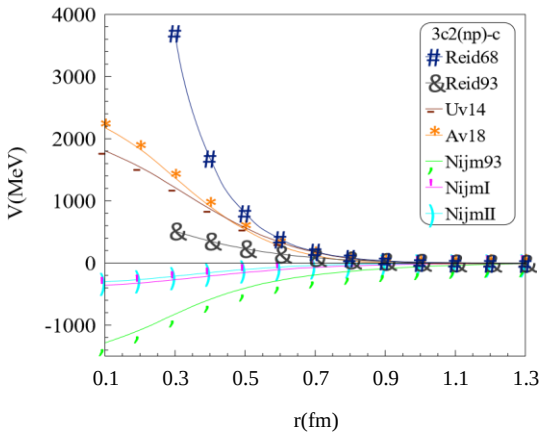
3c2(np)-c
Reid68
Reid93
Uv14
Av18
Nijm93
NijmI
NijmII
V(MeV)
r(fm)

***Fig. 3**. The central potentials of some potential forms in the states from J=0 up to J=9, for np system.*

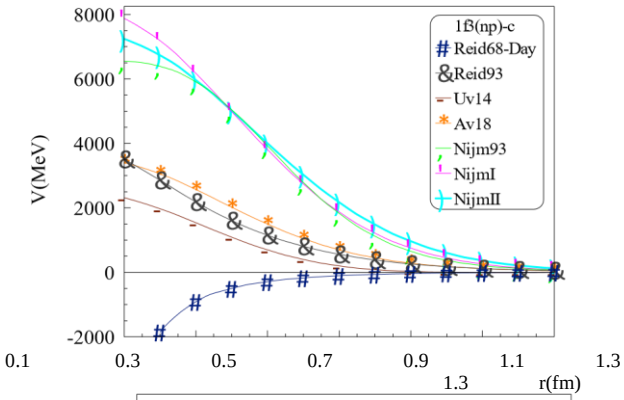
1f1(np)-c
Reid68-Day
Reid93
Uv14
Av18
Nijm93
NijmI
NijmII
V(MeV)
r(fm)

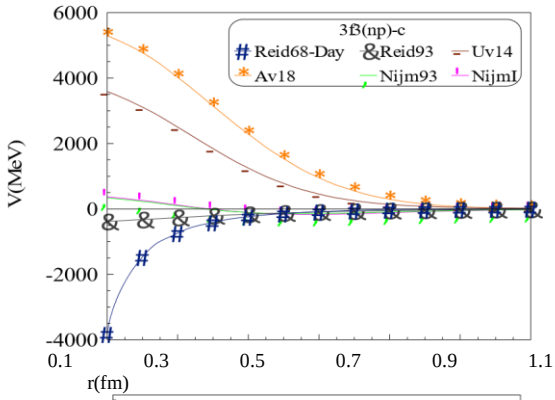
3f1(np)-c
Reid68-Day
Reid93
Uv14
Av18
Nijm93
NijmI
V(MeV)
r(fm)

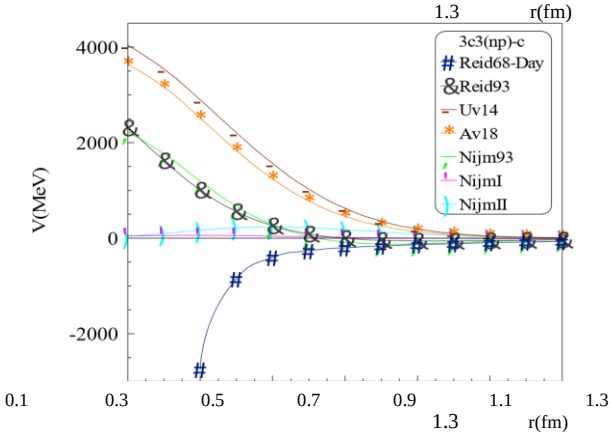
3c3(np)-c
Reid68-Day
Reid93
Uv14
Av18
Nijm93
NijmI
NijmII
V(MeV)
r(fm)

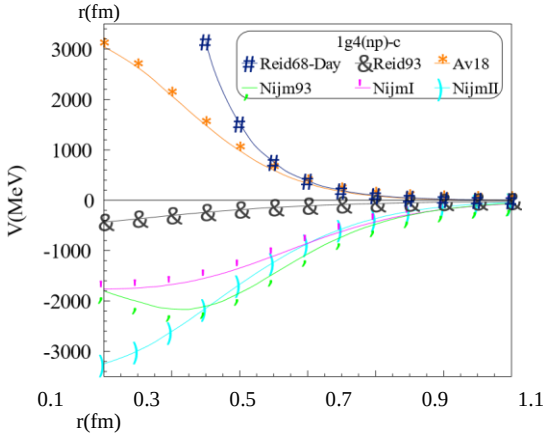
1g4(np)-c
Reid68-Day
Reid93
Av18
Nijm93
NijmI
NijmII
V(MeV)
r(fm)

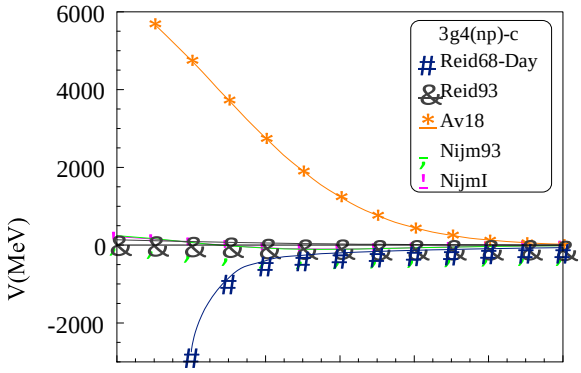
3g4(np)-c
Reid68-Day
Reid93
Av18
Nijm93
NijmI
V(MeV)

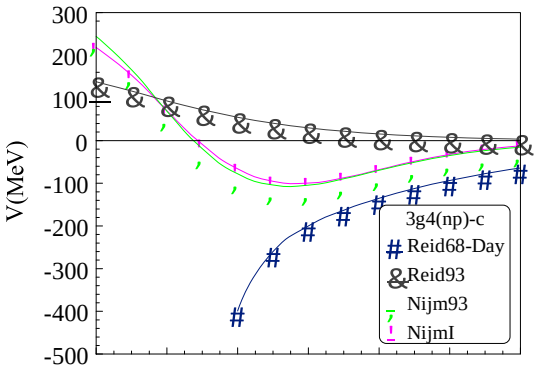
3g4(np)-c
Reid68-Day
Reid93
Nijm93
NijmI
V(MeV)

0.1 0.3 0.5 0.7 0.9 1.1 1.3 0.1 0.3 0.5 0.7 0.9 1.1

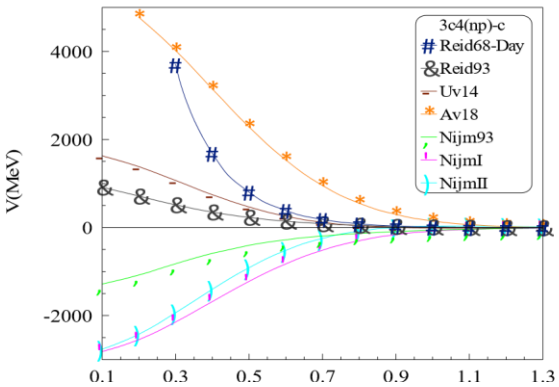

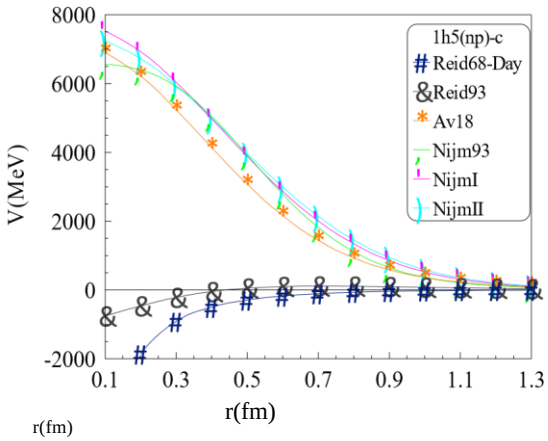

1.3 r(fm) r(fm) r(fm)

Fig. *3. Continuation.*

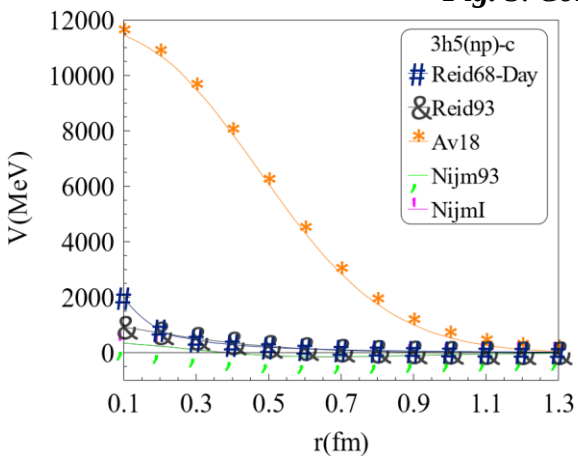

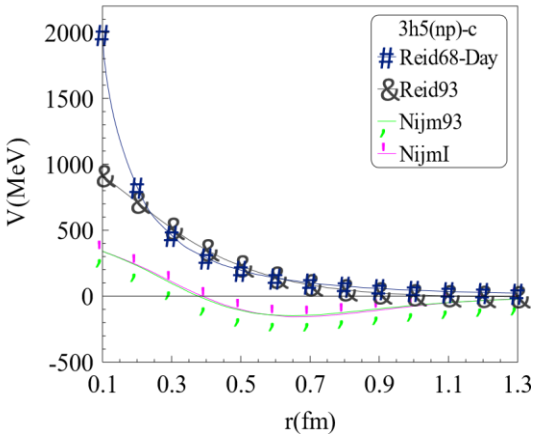

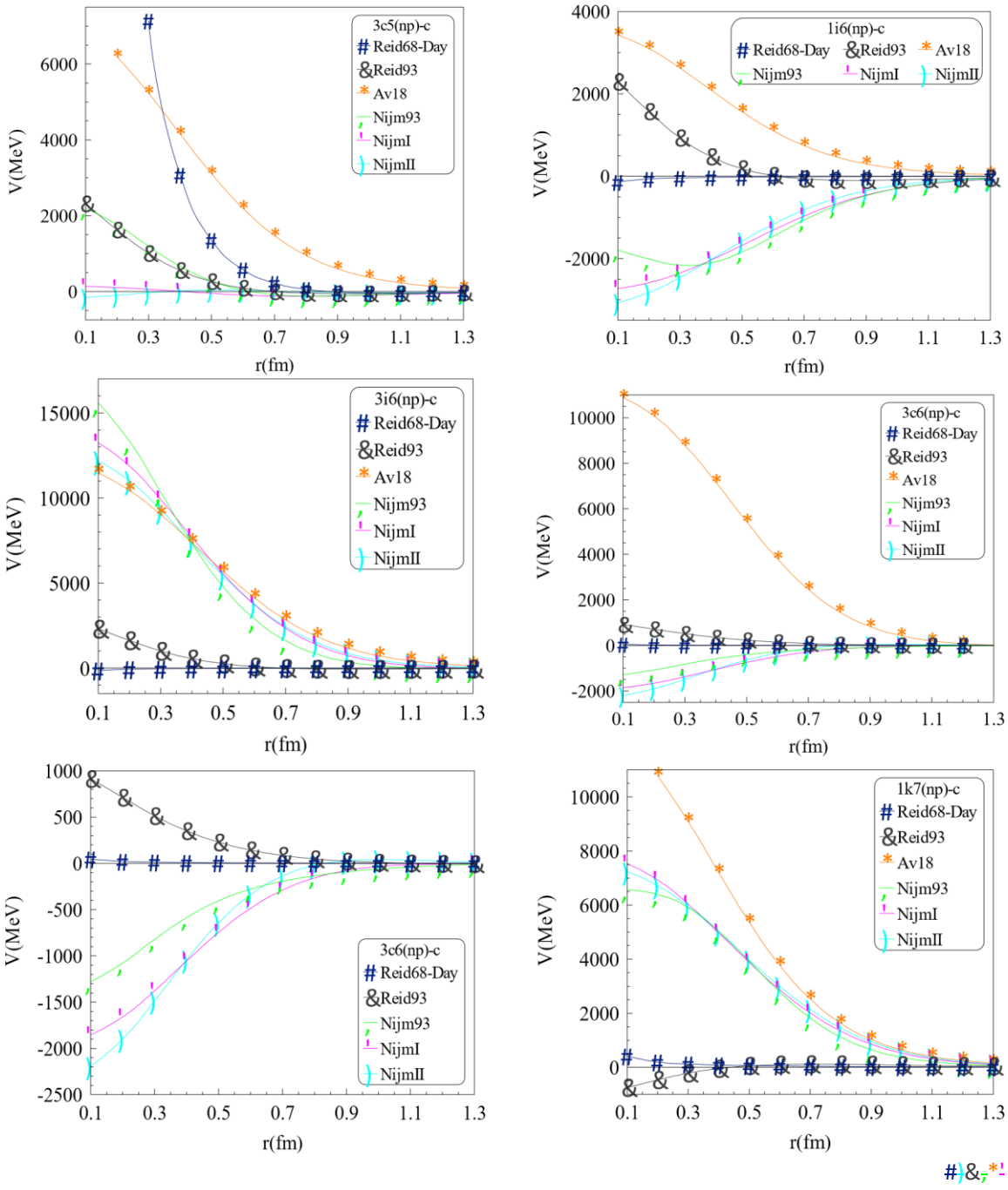

Fig. 3. *Continuation.*

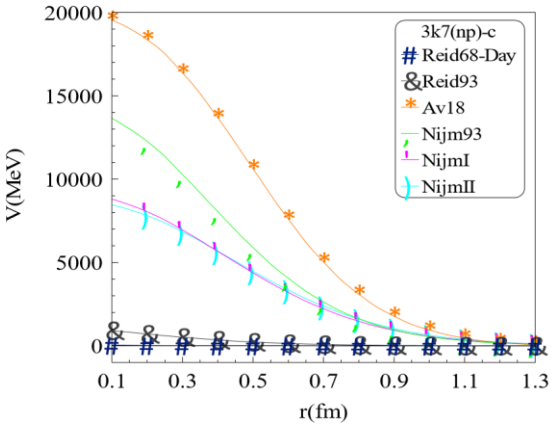
3k7(np)-c
Reid68-Day
Reid93
Av18
Nijm93
NijmI
NijmII
V(MeV)
r(fm)

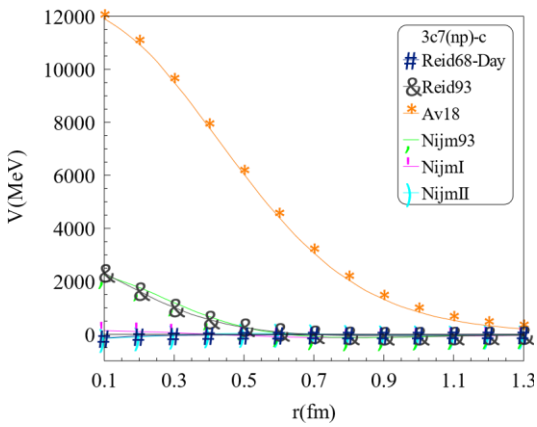
3c7(np)-c
Reid68-Day
Reid93
Av18
Nijm93
NijmI
NijmII
V(MeV)
r(fm)

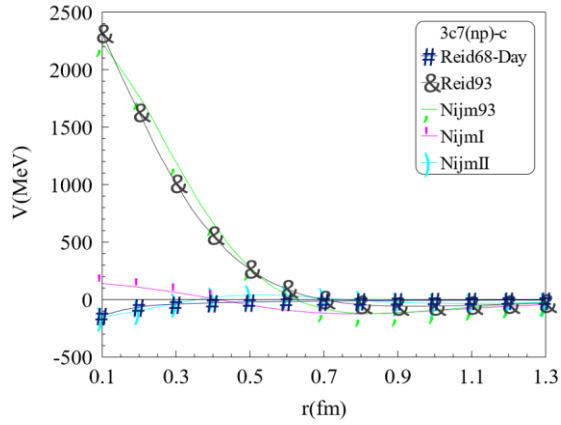
3c7(np)-c
Reid68-Day
Reid93
Nijm93
NijmI
NijmII
V(MeV)
r(fm)

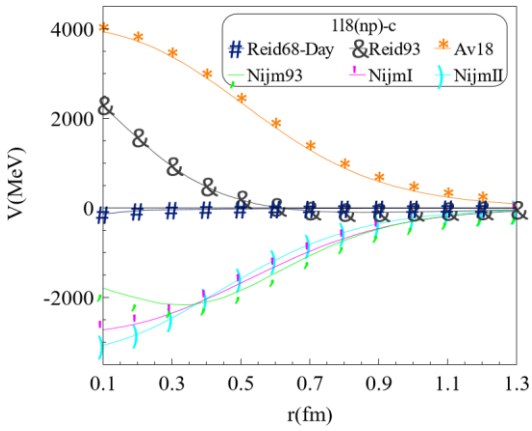
1l8(np)-c
Reid68-Day
Reid93
Av18
Nijm93
NijmI
NijmII
V(MeV)
r(fm)

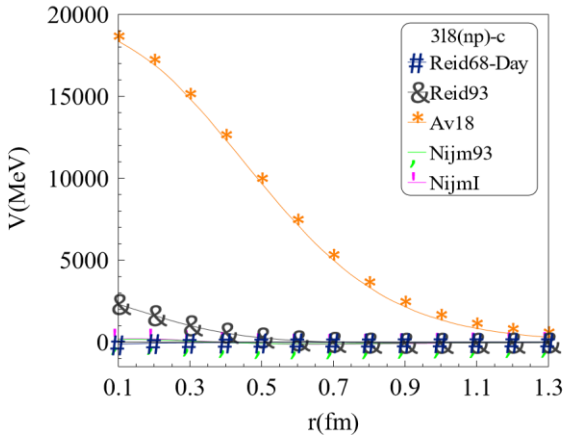
3l8(np)-c
Reid68-Day
Reid93
Av18
Nijm93
NijmI
V(MeV)
r(fm)

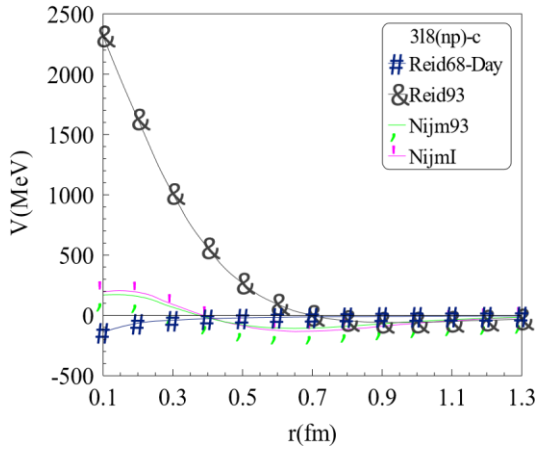
3l8(np)-c
Reid68-Day
Reid93
Nijm93
NijmI
V(MeV)
r(fm)

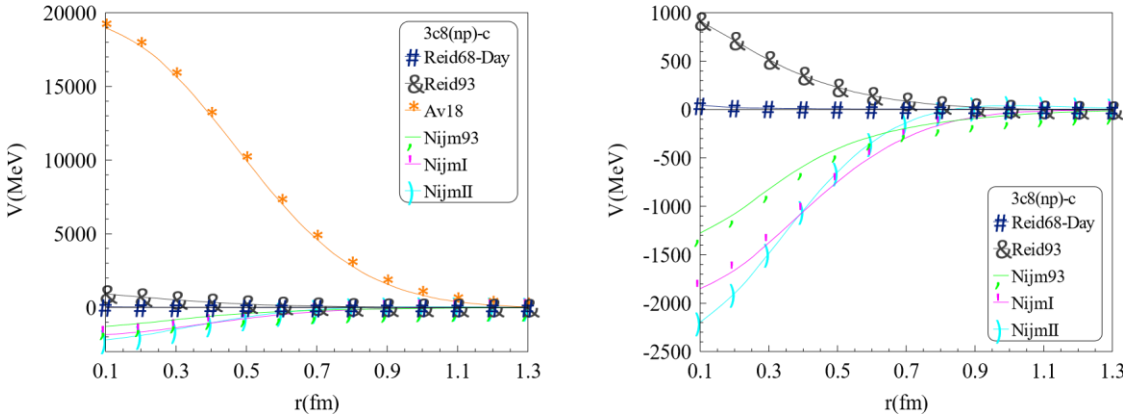

Fig .3. *Continuation.*

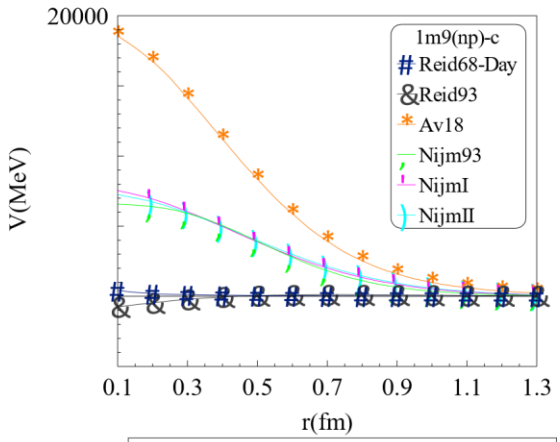
1m9(np)-c
Reid68-Day
&Reid93
* Av18
Nijm93
NijmI
NijmII
V(MeV)
r(fm)

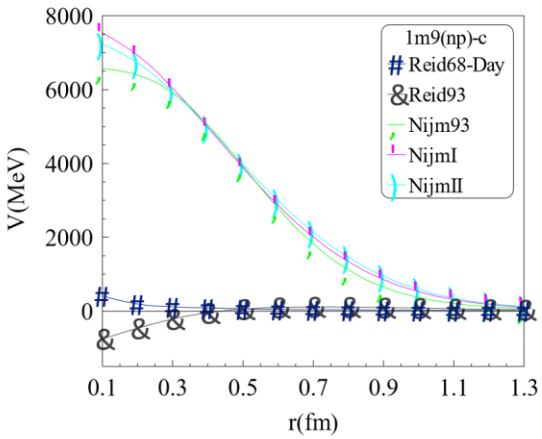
1m9(np)-c
Reid68-Day
&Reid93
Nijm93
NijmI
NijmII
V(MeV)
r(fm)

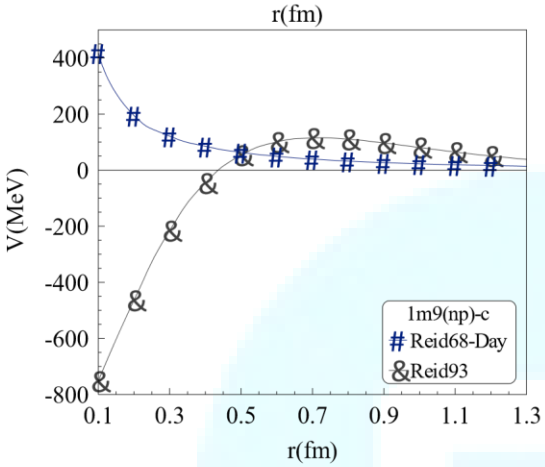
1m9(np)-c
Reid68-Day
&Reid93
V(MeV)
r(fm)

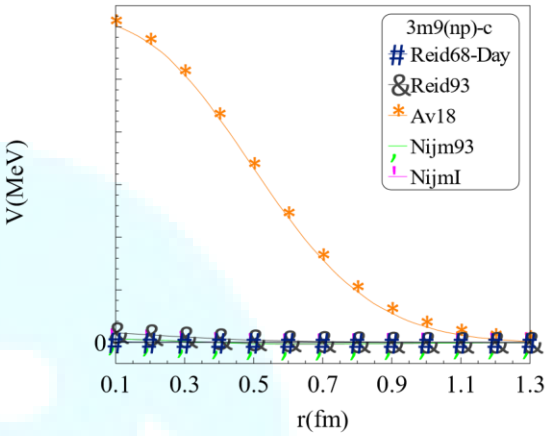
3m9(np)-c
Reid68-Day
&Reid93
* Av18
Nijm93
NijmI
V(MeV)
r(fm)

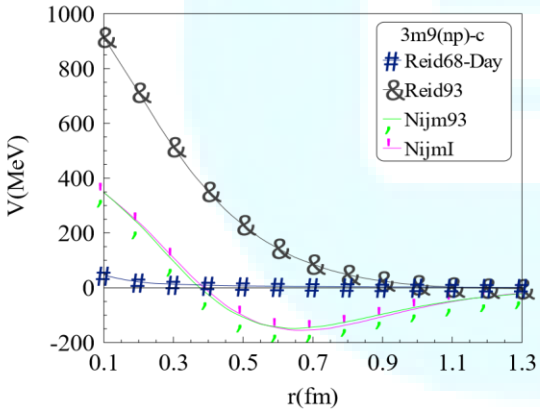
3m9(np)-c
Reid68-Day
&Reid93
Nijm93
NijmI
V(MeV)
r(fm)

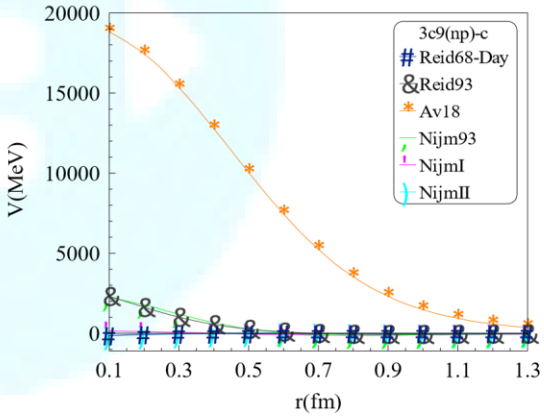
3c9(np)-c
Reid68-Day
&Reid93
* Av18
Nijm93
NijmI
NijmII
V(MeV)
r(fm)

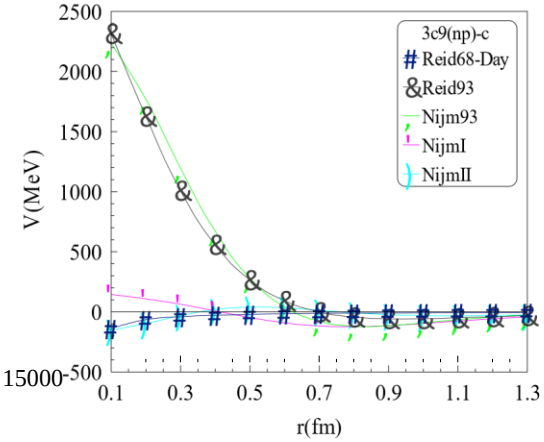
3c9(np)-c
Reid68-Day
&Reid93
Nijm93
NijmI
NijmII
V(MeV)
r(fm)

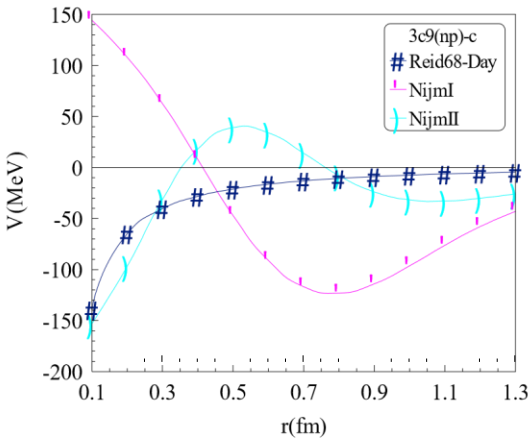
3c9(np)-c
Reid68-Day
NijmI
NijmII
V(MeV)
r(fm)

10000

),'

5000

0

-5000

1.3

30000

25000

#& 20000

15000

10000

5000

Fig .3. *Continuation.*

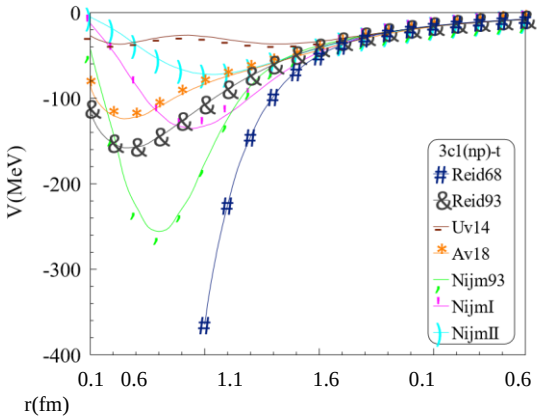
V(MeV)
r(fm)
3c1(np)-t
Reid68
Reid93
Uv14
Av18
Nijm93
NijmI
NijmII

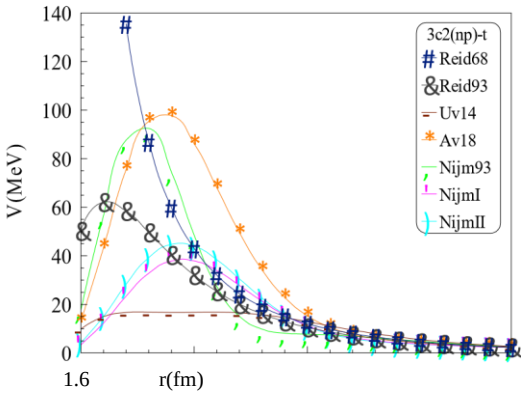
V(MeV)
r(fm)
3c2(np)-t
Reid68
Reid93
Uv14
Av18
Nijm93
NijmI
NijmII

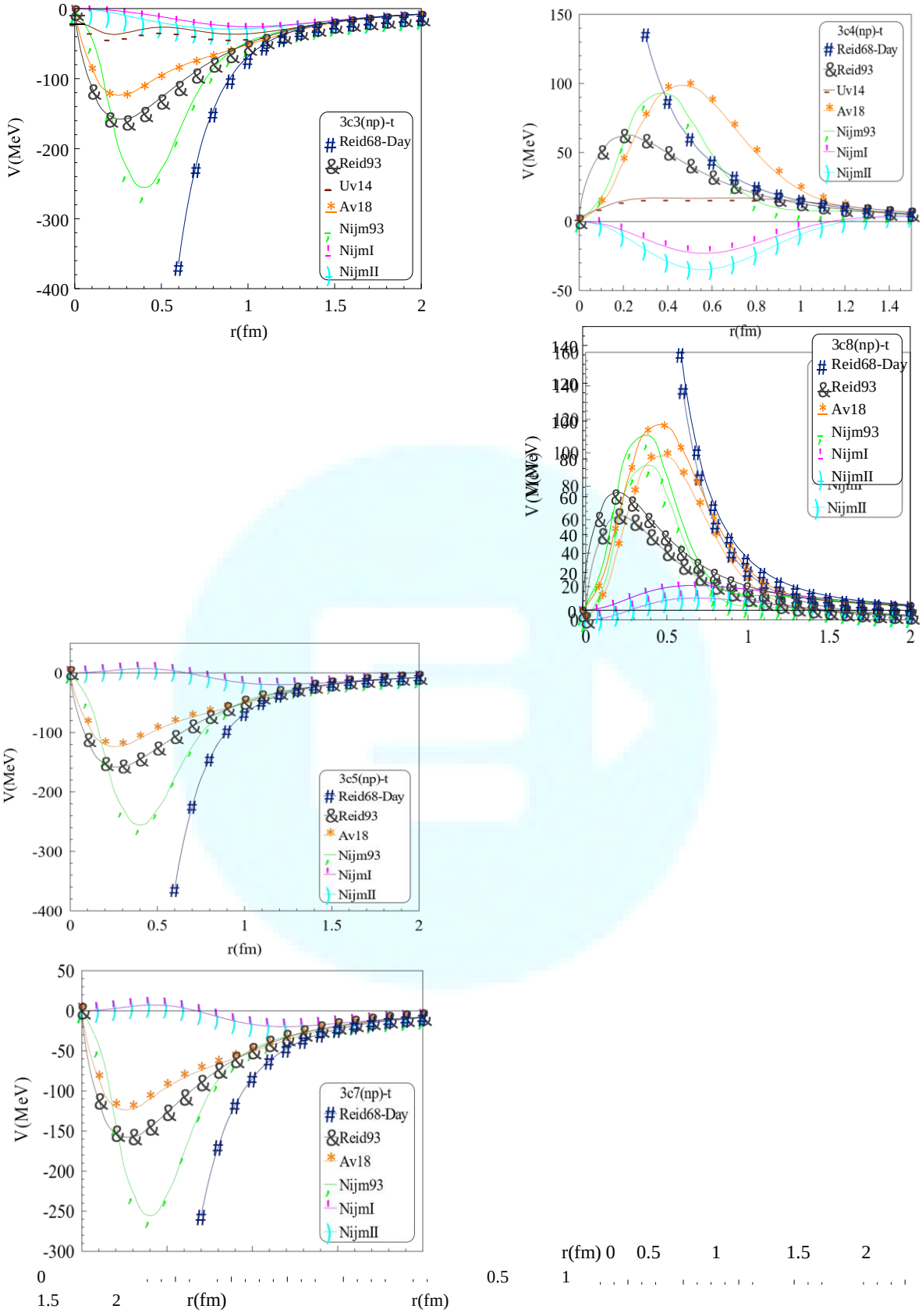

Fig. 4. *The tensor potentials of some potential forms in the states from J=1 up to J=8, for np system.*

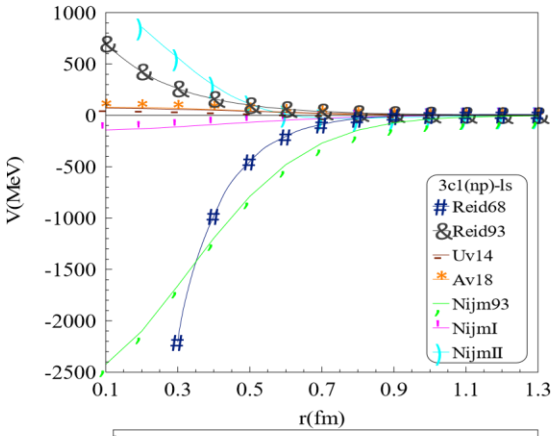
3c1(np)-ls
Reid68
Reid93
Uv14
Av18
Nijm93
NijmI
NijmII
V(MeV)
r(fm)

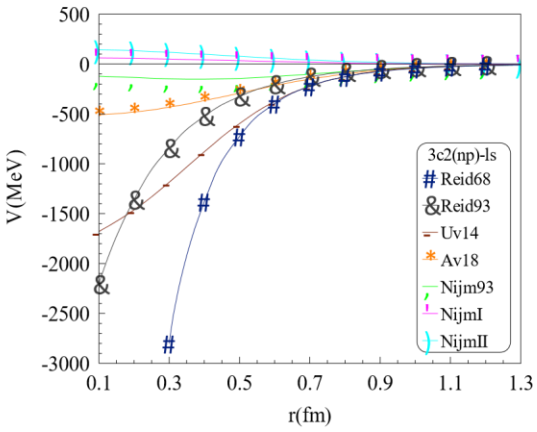
3c2(np)-ls
Reid68
Reid93
Uv14
Av18
Nijm93
NijmI
NijmII
V(MeV)
r(fm)

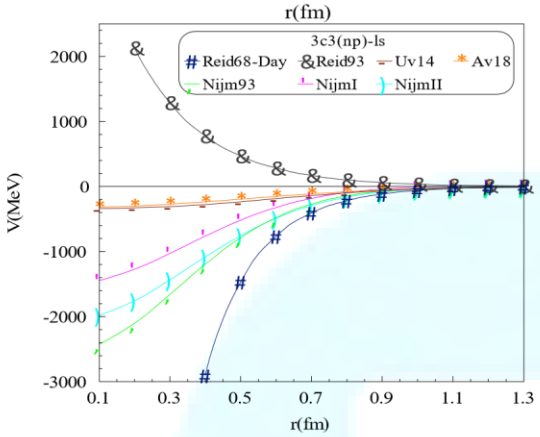
3c3(np)-ls
Reid68-Day
Reid93
Uv14
Av18
Nijm93
NijmI
NijmII
V(MeV)
r(fm)

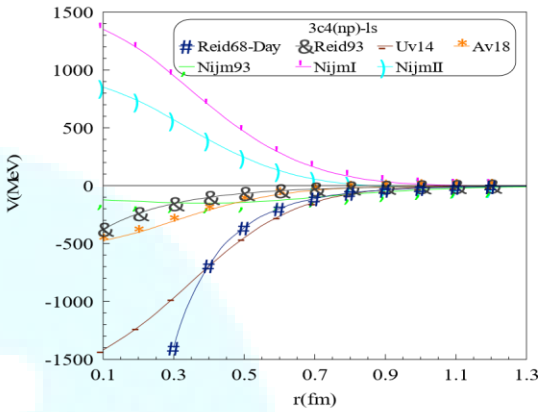
3c4(np)-ls
Reid68-Day
Reid93
Uv14
Av18
Nijm93
NijmI
NijmII
V(MeV)
r(fm)

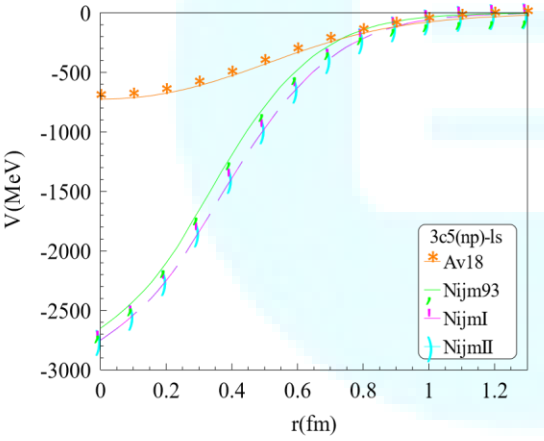
3c5(np)-ls
Av18
Nijm93
NijmI
NijmII
V(MeV)
r(fm)

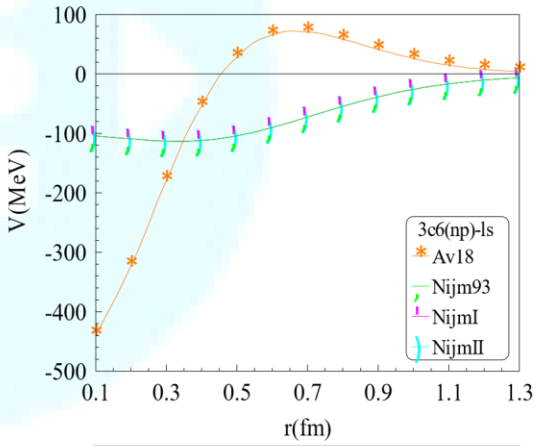
3c6(np)-ls
Av18
Nijm93
NijmI
NijmII
V(MeV)
r(fm)

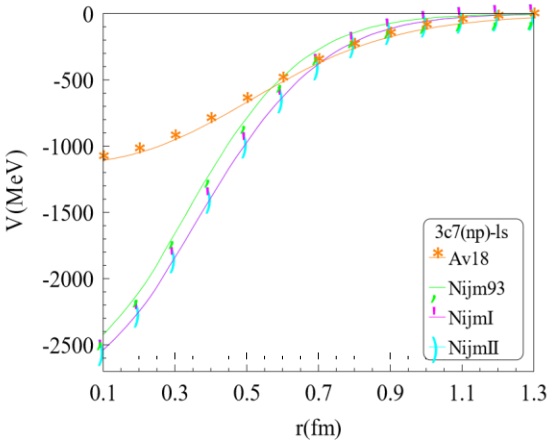
3c7(np)-ls
Av18
Nijm93
NijmI
NijmII
V(MeV)
r(fm)

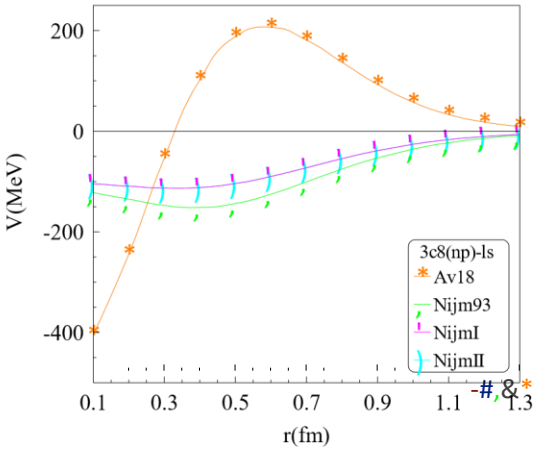
3c8(np)-ls
Av18
Nijm93
NijmI
NijmII
V(MeV)
r(fm)

Fig. 5. *The spin-orbit potentials of some potential forms in the states from J=1 up to J=8, for np system.*

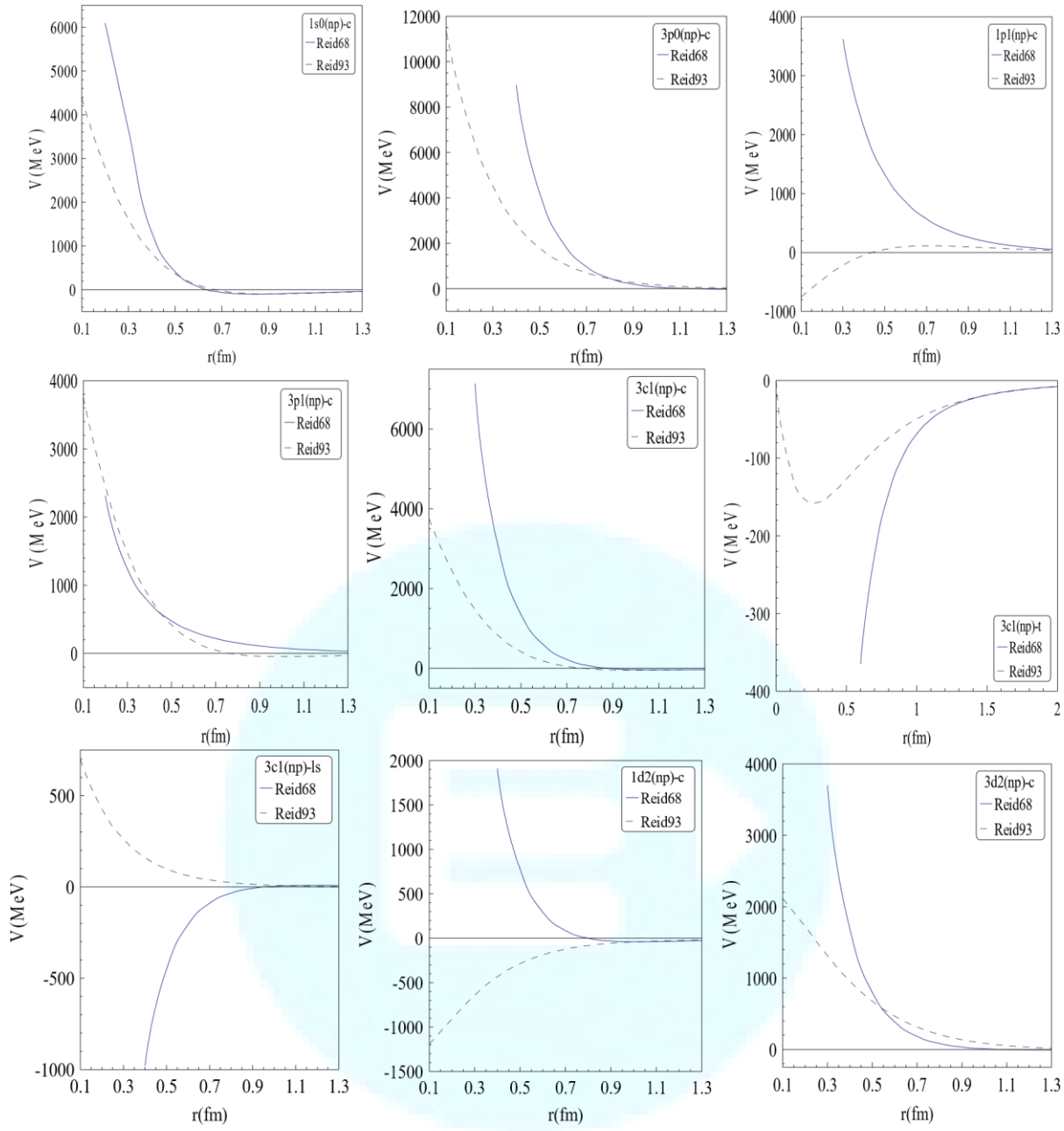
1s0(np)-c
Reid68
Reid93
V(MeV)
r(fm)
3p0(np)-c
Reid68
Reid93
V(MeV)
r(fm)
1p1(np)-c
Reid68
Reid93
V(MeV)
r(fm)
3p1(np)-c
Reid68
Reid93
V(MeV)
r(fm)
3c1(np)-c
Reid68
Reid93
V(MeV)
r(fm)
3c1(np)-t
Reid68
Reid93
V(MeV)
r(fm)
3c1(np)-ls
Reid68
Reid93
V(MeV)
r(fm)
1d2(np)-c
Reid68
Reid93
V(MeV)
r(fm)
3d2(np)-c
Reid68
Reid93
V(MeV)
r(fm)

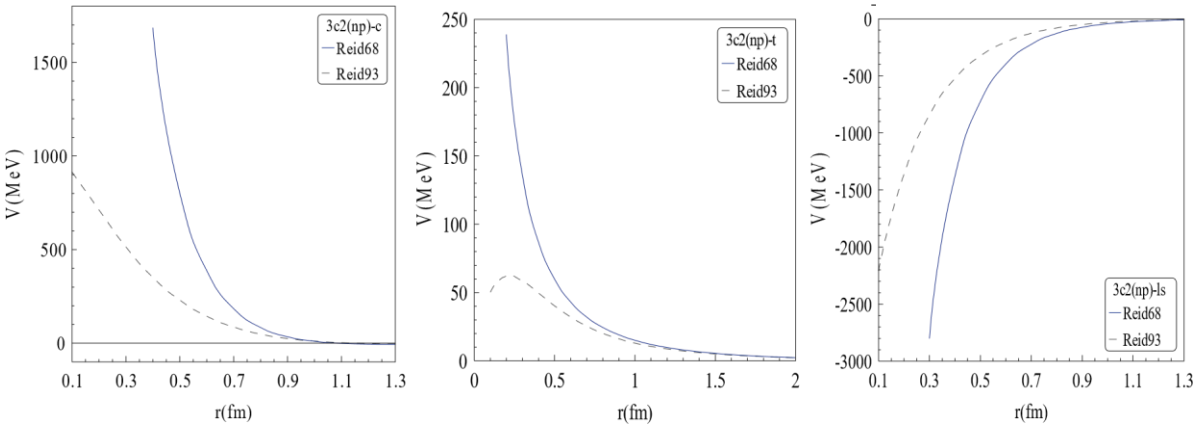

Fig. 6. *The comparison of central, tensor, and spin-orbit potentials of Reid68 and Reid93 , for the states from J=0 up to J=2, for np system.*

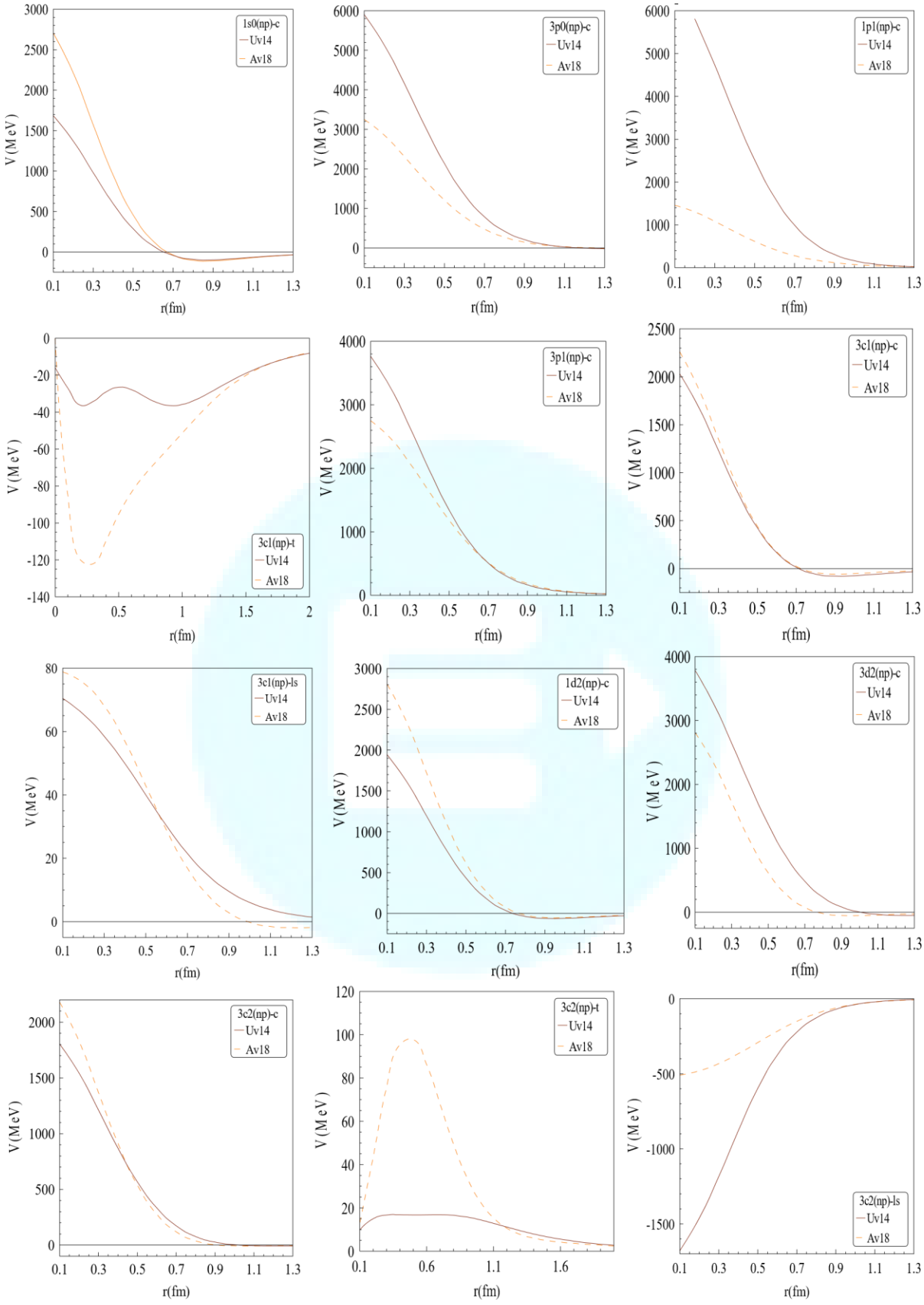
1s0(np)-c
Uv14
Av18
V(MeV)
r(fm)
3p0(np)-c
Uv14
Av18
V(MeV)
r(fm)
1p1(np)-c
Uv14
Av18
V(MeV)
r(fm)
3c1(np)-t
Uv14
Av18
V(MeV)
r(fm)
3p1(np)-c
Uv14
Av18
V(MeV)
r(fm)
3c1(np)-c
Uv14
Av18
V(MeV)
r(fm)
3c1(np)-ls
Uv14
Av18
V(MeV)
r(fm)
1d2(np)-c
Uv14
Av18
V(MeV)
r(fm)
3d2(np)-c
Uv14
Av18
V(MeV)
r(fm)
3c2(np)-c
Uv14
Av18
V(MeV)
r(fm)
3c2(np)-t
Uv14
Av18
V(MeV)
r(fm)
3c2(np)-ls
Uv14
Av18
V(MeV)
r(fm)

Fig.7. *The comparison of central, tensor, and spin-orbit potentials - of UV_{14} and AV_{18} potentials reduced to Reid potential, for the states from J=0 up to J=2, for np system.*

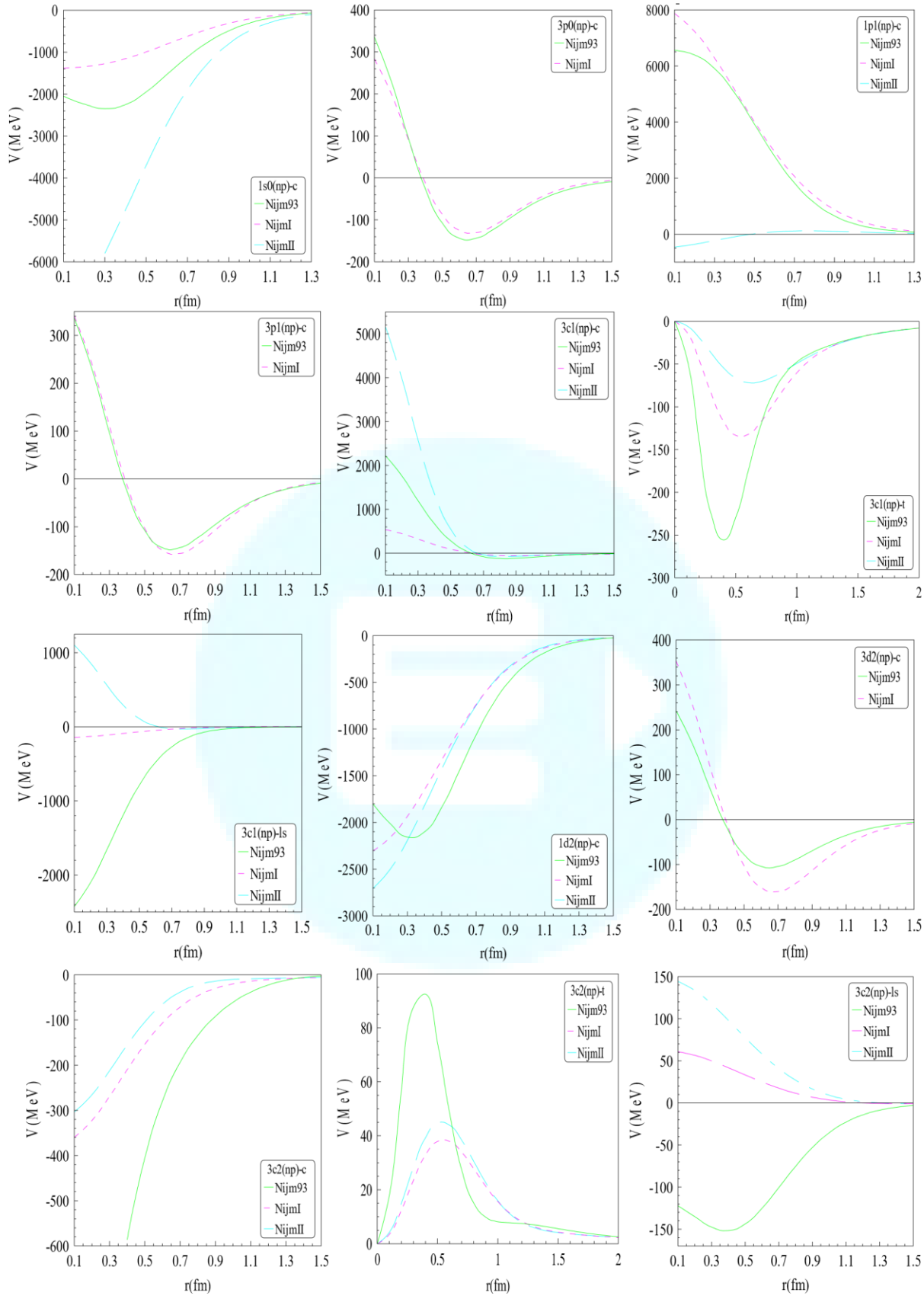

Fig.8. *The comparison of central, tensor, and spin-orbit potentials of Nijm93, NijmI, and NijmII reduced to Reid potential, for the states from J=0 up to J=2, for np system.*

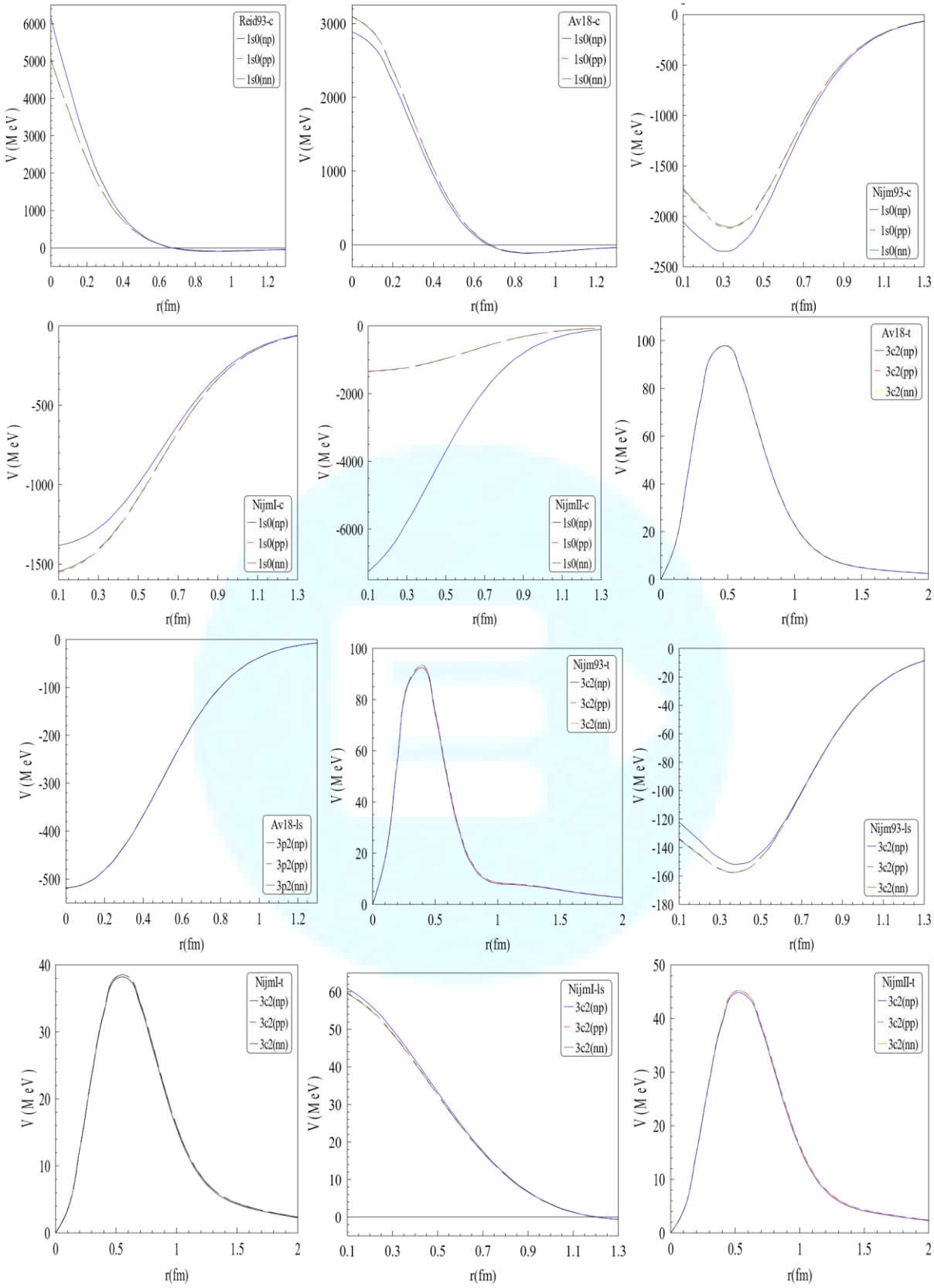

Fig. 9. *The charge-dependence of the charge-dependent potentials reduced to Reid potential, the states* ${}^1S_0$ *(central) and also* ${}^3P_2 - {}^3F_2(3C2)$ *(tensor and spin-orbit).*

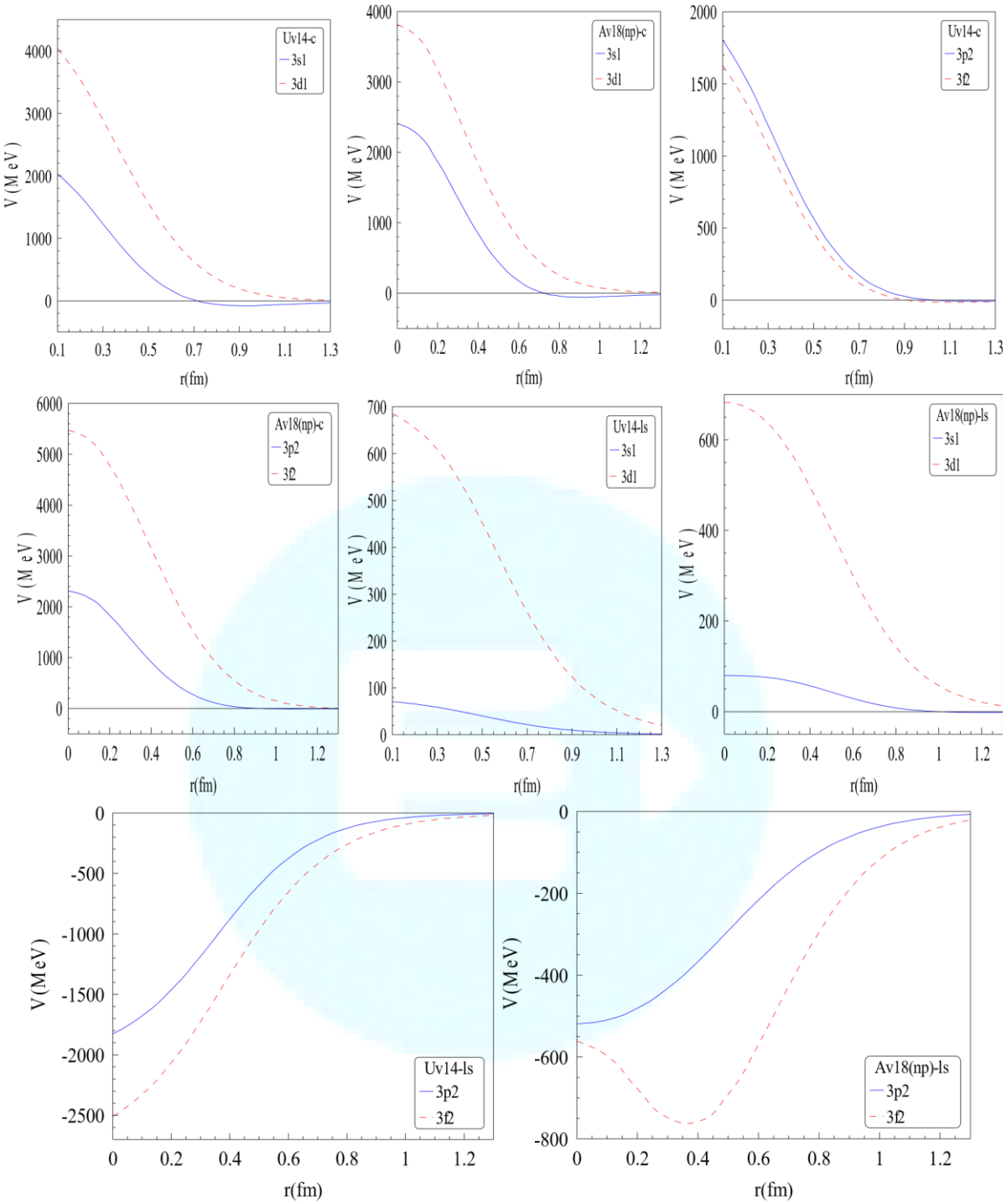

Fig. 10. *The comparison of* ${}^3S_1$ (□= 0), ${}^3D_1$ (□= 2)*and also* ${}^3P_2$ (□=1) , ${}^3F_2$ (□= 3) *central and spin-orbit potentials of the* UV_{14} *and* AV_{18} *potentials reduced to Reid potential, for np system.*